ISSN 1606-867X (Print)
ISSN 2687-0711 (Online)
Condensed Matter and Interphases
Kondensirovannye Sredy i Mezhfaznye Granitsy
https://journals.vsu.ru/kcmf/

Original articles

Research article
https://doi.org/10.17308/kcmf.2024.26/12214

Probing molecular interactions, electronic properties, and reactivity of monoamine neurotransmitters in different protonation states via quantum chemical investigation

Y. H. Azeez[1], K. A. Othman[2], R. A. Omer[2,3], A. F. Qader[2]✉

[1]University of Halabja, College of Science, Department of Physics, Halabja, Iraq

[2]Department of Chemistry, Faculty of Science and Health, Koya University, Danielle Mitterrand Boulevard, Koya KOY45, Kurdistan Region – F.R., Iraq

[3]Knowledge University, College of Pharmacy, Department of Pharmacy,

Erbil 44001, Iraq

Abstract

Amphetamine, dopamine, norepinephrine, serotonin, and tryptamine are a group of monoamine neurotransmitters that regulate diverse brain functions. This work examined these compounds' neutral, protonated, and deprotonated, structural, energetic, and optical properties using quantum chemistry methods. Noncovalent interactions (NCI) and reduced density gradient (RDG) investigations revealed weak intermolecular forces and electron density distribution. The RDG values were observed to span from 0.12 to 0.43, indicating varying degrees of repulsion or attraction. The hydrogen bonding patterns and their strength and nature were also investigated using the Atoms in Molecules (AIM) and B3LYP methods. The quantification was done using ∇^2 ρ(r), H(r), and energy density values, which showed a variation from -0.014 to 0.026 Hartree/Bohr3, reflecting covalent or electrostatic interactions. A comparison was made between the compounds based on their physical and chemical attributes, such as polar surface area (ranging from 41.81 to 86.71 Å^2), rotatable bonds (which were identical), and proton affinity (a measure of stability). Lewis structures and natural bond orbital (NBO) analysis showed resonance and electron delocalization. The study also examined their molecular orbitals (MOs) and found that protonation and deprotonation could significantly change their electronic characteristics, including the energies of the highest occupied (HOMO) and lowest unoccupied (LUMO), the energy gap, and the shape and size of their lobes. The nonlinear optical properties were also assessed, affected by polarizability and hyperpolarizability indices, ranging from 2.267 a.u. (Dopamine) to 7.891 a.u. (Protonated Serotonin). These properties pointed to the applications of these compounds in optical devices.

Keywords: Quantum chemistry, Molecular interactions, Monoamine neurotransmitters, electronic properties, and Protonation states

Acknowledgments: We would like to thank the heads of the chemistry departments at Koya University for their support.

For citation: Azeez Y. H., Othman Kh. A., Omer R. A., Qader A. F. Probing molecular interactions, electronic properties, and reactivity of monoamine neurotransmitters in different protonation states via quantum chemical investigation. *Condensed Matter and Interphases.* 2024;26(3): 379–406. https://doi.org/10.17308/kcmf.2024.26/12214

Для цитирования: Азиз Ю. Х., Османа Х. А., Омер Р. А., Кадер А. Ф. Квантово-химическое исследование молекулярных взаимодействий, электронных свойств и реакционной способности моноаминных нейромедиаторов в различных состояниях протонирования. *Конденсированные среды и межфазные границы*. 2024;26(3): 379–406. https://doi.org/10.17308/kcmf.2024.26/12214

✉ Aryan F. Qader, aryan.qader@koyauniversity.org

1. Introduction

Amphetamines, a class of psychoactive compounds, exert profound effects on the central nervous system. Notably, amphetamine, a potent stimulant, triggers the release of key neurotransmitters-dopamine, norepinephrine, and serotonin-crucial for mood, attention, and physiological processes. Dopamine relates to pleasure, norepinephrine to alertness, and serotonin to emotional well-being. Tryptamine, a fundamental neurotransmitter component, underscores their interconnected role in cognition and sensation, affecting normal brain function and psychoactive substance effects [1–5]. Noncovalent interactions (NCIs), encompassing weak molecular forces, hold vast significance across chemistry, biology, and material science, notably in drug discovery for optimized interactions [6]. Recent strides in methodologies like Reduced Density Gradient (RDG) analysis and Noncovalent Interaction (NCI) indices are pivotal for deciphering these interactions and enhancing tailored drug-target binding for therapeutic efficacy. The Reduced Density Gradient (RDG) method, rooted in electron density, unveils spatial distribution insights for Non-covalent interactions like hydrogen bonds and van der Waals forces, refining drug binding and selectivity. This study employs RDG and NCI methods to explore Non-covalent interactions, spotlighting their role in drug design. Objectives encompass characterizing interactions, assessing protonation effects, and examining resulting molecular properties, promising refined drug design for potent therapeutic agents [7–9]. The investigation extends to topological parameters via the Atoms in Molecules (AIM) approach, vital for understanding drug-receptor interactions and enhancing binding affinity [10, 11]. By utilizing advanced computational techniques, including Density Functional Theory (DFT), this study uncovers the distribution of attractive/repulsive forces depicted through RDG scatter plots and topological parameters [12]. The exploration also delves into nonlinear optical properties (NLO) and quantum parameters, offering multifaceted insights [13, 14].

This study delves into the intricate world of molecular interactions, bridging neurochemistry and computational chemistry to advance our comprehension of the human mind and pharmaceutical development.

2. Computational Details

In this study, the computational investigations were conducted using the Gaussian software package, a prominent suite of quantum chemistry tools [15–17]. The Density Functional Theory (DFT) calculations used the accurate 6-31G(d,p) and 6-311++G(d,p) basis sets, enabling a precise exploration of molecular interactions, electron densities, and energy profiles. These aspects are crucial for optimizing drug-receptor binding and enhancing the understanding of non-covalent interactions [18–20].

3. Results and discussion

3.1. RDG and NCI Analysis

Noncovalent interactions (NCI) and reduced density gradient (RDG) studies are novel methodologies used for the characterization of weak intermolecular interactions [55–58]. The NCI index is used for characterizing intermolecular interactions and evaluating the characteristics of weak interactions. The NCI index is derived from the reduced density gradient (RDG) and provides further support for non-covalent interactions. The reduced density gradient (RDG) is a fundamental dimensionless quantity that includes the density and its initial derivative . The colorful RDG scatter plots were produced using the Multiwfn program, whereas the 3D isosurface was shown employing the VMD software [21, 22]. The NCI studies were conducted using an isosurface threshold of 0.5. The isosurface range for the Reduced Density Gradient (RDG) extends from –0.035 to 0.02 atomic units. Fig. 1 displays the two-dimensional representation of the reaction-diffusion grid (RDG) plots, as well as the three-dimensional isosurface.

The determination of the electron density of the sign(k2)q peaks concerning RDG provides valuable insights into the characteristics and intensity of the molecular interactions. Within the molecular system, the color blue shows attractive interactions, whereas the colour red signifies repulsive interactions. The sign of the product between the sign of $\lambda 2$ and the charge $\rho(r)$ is crucial in determining the characteristics of the interaction. Specifically, when the sign of $\lambda 2$

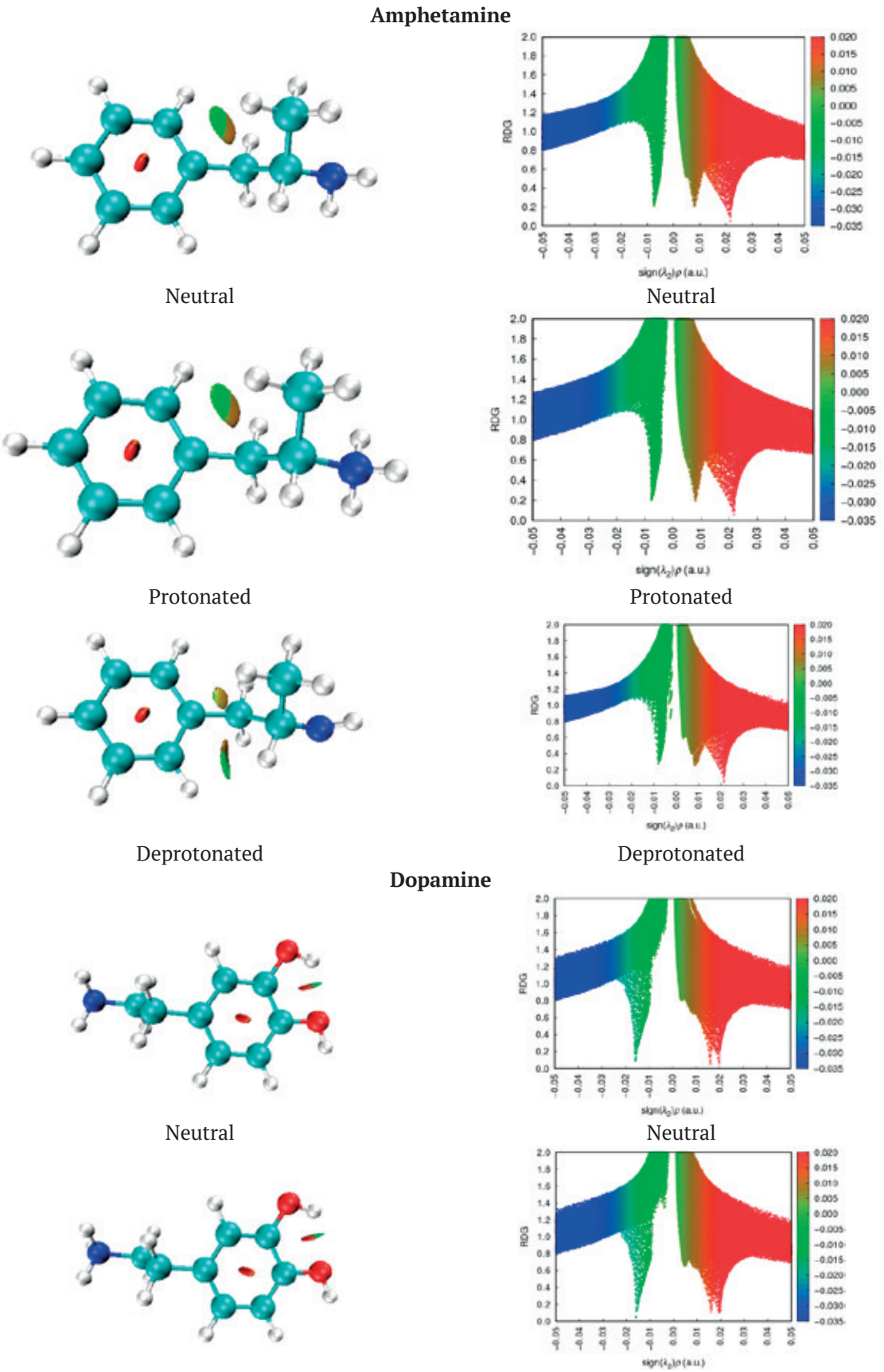

Fig. 1. Reduced Density Gradient (RDG) analysis showing weak and strong interaction of all compounds

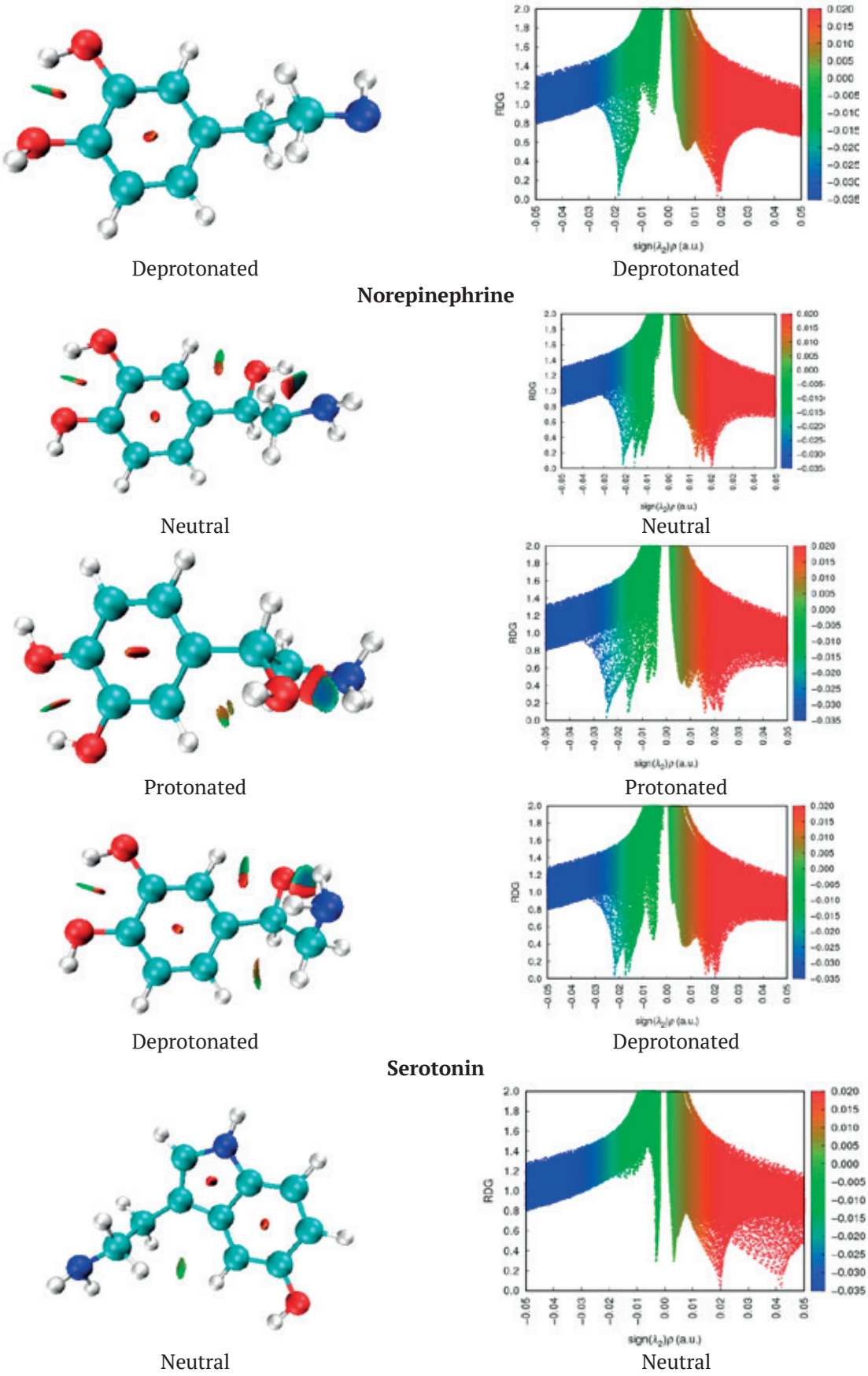
Deprotonated
Deprotonated
Norepinephrine
Neutral
Neutral
Protonated
Protonated
Deprotonated
Deprotonated
Serotonin
Neutral
Neutral

Fig. 1.

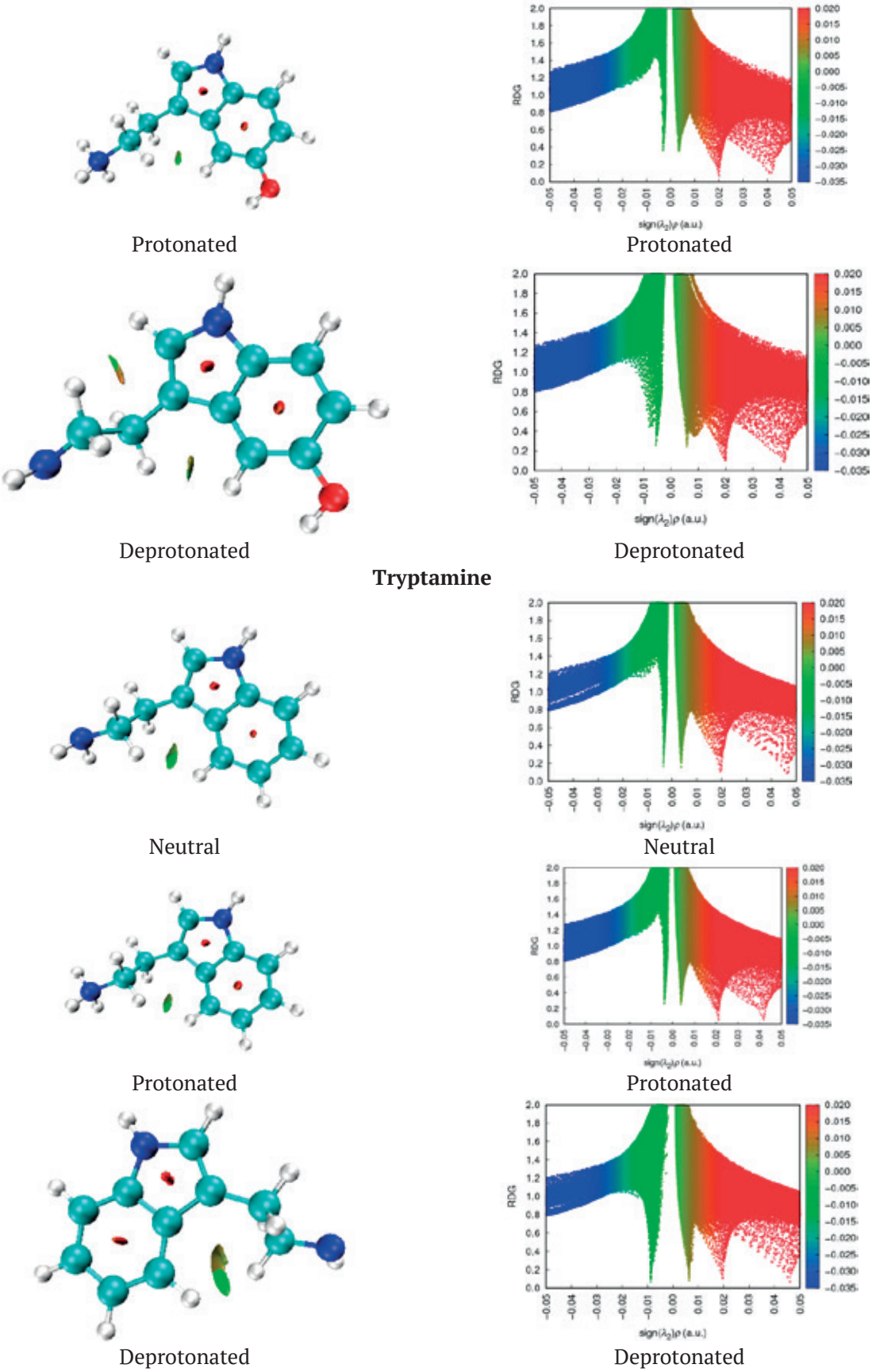
Protonated
Protonated
Deprotonated
Deprotonated
Tryptamine
Neutral
Neutral
Protonated
Protonated
Deprotonated
Deprotonated

Fig. 1.

ρ(r) is negative, it signifies a repulsive interaction that is bonded. Conversely, when the sign (λ2) ρ is positive, along with the corresponding symbol, it shows a repulsive interaction that is non-bonded.

The scatter graphs of the RDG complexes are shown on the right side of Fig. 1. As seen on the left side of Fig. 1, the color red is assigned to denote strong repulsion resulting from steric effects, blue is used to show hydrogen bonding interactions, and green is employed to signify van der Waals interactions [23, 24]. As seen on the left side of Fig. 1, the blue coloration signifies the occurrence of hydrogen bonding. The green coloration correlates to van der Waals interactions, while the red coloration shows steric or cyclic effects. It is observed that all deprotonated compounds possess a low density and have a limited hydrogen interaction. Conversely, all protonated compounds show a larger density and display hydrogen bond interactions.

Serotonin and tryptamine have a pronounced repulsive behavior compared to other compounds, as seen by their red color in Fig. 1. The existence of a weak hydrogen bond interaction, together with additional contacts between the two hydrogen atoms (H–H), is shown by the observation of a green-colored isosurface for the serotonin and tryptamine complex. This green-colored isosurface may be attributed to van der Waals interactions. The identification of this isosurface position suggests the existence of van der Waals interactions.

3.2. Topological parameters

Using the atoms in molecules (AIM) analysis is a widely used approach for the detection and characterization of non-covalent interactions present in molecular systems, particularly emphasizing intra- and intermolecular hydrogen bonding. The determination of hydrogen bonds in molecular complexes is accomplished by conducting a thorough examination of electron density using topological techniques [25–28]. The B3LYP [29, 30] technique was used to calculate the topological characteristics, such as the Laplacian of electron density and the electron density, potential energy density, and ellipticity at bond critical sites (BCP). The computations have been succinctly presented in Table 1, while Fig. 2 provides a visual representation of the BCP.

Based on the findings presented in reference [27], the quantification of hydrogen bond interaction can be determined using the following criteria: weak hydrogen bonding is shown when the second derivative of the electron density regarding the distance is positive and the value of the Hamiltonian (H(r)) is positive; medium hydrogen bonding is categorized by a positive and a negative H(r); and strong hydrogen bonding is classified by a negative and a negative H(r).

The strong covalent connection between oxygen and hydrogen is shown by the significant negative values for O1-H21(–2.170) for protonated dopamine, as displayed in Table 1 and Fig. 2.

If the energy density at the critical sites is negative (HBCPs < 0), the hydrogen bond exhibits a covalent nature. Conversely, if the energy density is positive (HBCPs > 0), the hydrogen bond has an electrostatic character.

3.3. Drug likeness

Table 2 succinctly compares the physico-chemical attributes of five compounds – Amphetamine, dopamine, norepinephrine, serotonin, and tryptamine - in neutral, protonated, and deprotonated forms, shedding light on their potential utility in drug design. Notably, norepinephrine and dopamine exhibit a relatively higher number of hydrogen bond donors and acceptors compared to the expected range of <5, suggesting their propensity for strong interactions [31]. Norepinephrine boasts the largest polar surface area (PSA) of 86.71 Å², indicative of extensive interaction potential, while Tryptamine possesses a smaller PSA of 41.81 Å², suggesting a more focused interaction profile [32]. The variations in molecular weight among the compounds reflect Norepinephrine's relatively higher mass and Amphetamine's and Dopamine's lighter nature, potentially affecting their absorption and distribution properties [33]. Interestingly, all compounds share the same number of rotatable bonds (2), showing comparable flexibility [34]. The higher molar refractivity observed in dopamine and tryptamine implies their favorable interaction with polar environments [35]. Upon protonation, hydrogen bonding properties remain relatively stable across the compounds, with minor decreases in PSA values and minimal changes in molecular

Table 1. Topological parameters (all in a.u) at the bond critical point (BCP) of title compound [Electron density (, Laplacian of electron density (, and Ellipticity)], The units of V, G, and H are in a.u. For a – in a protonated state, and b – in a deprotonated state

1	2	3	4	5	6	7
a						
Amphetamine						
Связи				V	G	H
C2 – H11	0.295	−1.088	0.028	−0.346	0.037	−0.309
C3 – H12	0.283	−0.979	0.011	−0.331	0.043	−0.288
C3 – H13	0.283	−0.982	0.010	−0.332	0.043	−0.289
C5 – H16	0.282	−0.987	0.016	−0.331	0.042	−0.289
C5 – H14	0.287	−1.049	0.010	−0.340	0.039	−0.301
C5 – H15	0.280	−0.976	0.017	−0.328	0.042	−0.286
C6 – H17	0.288	−1.013	0.033	−0.344	0.045	−0.299
C7 – H18	0.289	−1.031	0.026	−0.345	0.043	−0.301
N1 – H19	0.336	−1.852	0.004	−0.539	0.038	−0.501
N1 – H20	0.336	−1.850	0.004	−0.539	0.038	−0.501
C8 – H21	0.292	−1.061	0.023	−0.349	0.042	−0.307
C9 – H22	0.292	−1.059	0.027	−0.350	0.042	−0.307
C10 – H23	0.292	−1.062	0.025	−0.349	0.042	−0.308
N1 – H24	0.336	−1.848	0.004	−0.538	0.038	−0.500
Dopamine						
N3 – H23	0.335	−1.851	0.003	0.500	0.000	0.500
C4 – H13	0.283	−0.983	0.011	0.288	0.000	0.288
C6 – H14	0.292	−1.086	0.031	0.308	0.000	0.308
C6 – H15	0.293	−1.089	0.031	0.308	0.000	0.308
C7 – H16	0.288	−1.021	0.036	0.300	0.000	0.301
C8 – H17	0.289	−1.030	0.027	0.301	0.000	0.301
C10 – H18	0.289	−1.032	0.029	0.302	0.000	0.302
N3 – H19	0.335	−1.853	0.003	0.501	0.000	0.501
N3 – H20	0.336	−1.853	0.003	0.501	0.000	0.501
O1 – H21	0.366	−2.170	0.021	0.601	0.001	0.602
O2 – H22	0.367	−2.166	0.019	0.602	0.001	0.603
Norepinephrine						
O1 – H24	0.025	0.128	0.320	−0.028	0.030	0.002
C5 – H13	0.289	−1.033	0.027	−0.332	0.037	−0.295
C7 – H14	0.292	−1.089	0.028	−0.344	0.036	−0.308
C7 – H15	0.293	−1.092	0.029	−0.345	0.036	−0.309
C8 – H16	0.290	−1.034	0.034	−0.348	0.045	−0.303
C9 – H17	0.289	−1.038	0.023	−0.345	0.043	−0.302
C11 – H18	0.290	−1.034	0.030	−0.346	0.044	−0.302
O1 – H19	0.363	−2.165	0.020	−0.658	0.058	−0.599
N4 – H20	0.337	−1.856	0.003	−0.541	0.039	−0.503
N4 – H24	0.326	−1.815	0.002	−0.522	0.034	−0.488
N4 – H21	0.337	−1.860	0.003	−0.542	0.038	−0.503
O2 – H22	0.366	−2.171	0.020	−0.659	0.058	−0.601
O3 – H23	0.367	−2.168	0.019	−0.662	0.060	−0.602

Table 1.

1	2	3	4	5	6	7
Serotonin						
C6 – H14	0.284	−0.986	0.012	−0.332	0.043	−0.289
C11 – H21	0.290	−1.044	0.023	−0.347	0.043	−0.304
C11 – C13	0.316	−0.822	0.507	−0.439	0.117	−0.322
C13 – H22	0.293	−1.065	0.026	−0.350	0.042	−0.308
C6 – H15	0.282	−0.974	0.013	−0.328	0.042	−0.286
C8 – H16	0.290	−1.076	0.026	−0.345	0.038	−0.307
N2 – H17	0.348	−1.841	0.057	−0.579	0.059	−0.520
C9 – H18	0.292	−1.087	0.032	−0.344	0.036	−0.308
C9 – H19	0.293	−1.090	0.032	−0.344	0.036	−0.308
C10 – H20	0.282	−0.964	0.045	−0.340	0.050	−0.290
N3 – H23	0.335	−1.851	0.003	−0.538	0.038	−0.501
N3 – H24	0.336	−1.853	0.004	−0.539	0.038	−0.501
O1 – H25	0.372	−2.146	0.021	−0.665	0.064	−0.601
N3 – H26	0.336	−1.853	0.003	−0.539	0.038	−0.501
C6 – H14	0.284	−0.986	0.012	−0.332	0.043	−0.289
Tryptamine						
C5 – H13	0.284	−0.987	0.012	−0.332	0.043	−0.290
C10 – H20	0.290	−1.036	0.029	−0.346	0.044	−0.303
C11 – H21	0.291	−1.050	0.025	−0.348	0.043	−0.305
C12 – H22	0.292	−1.057	0.024	−0.349	0.042	−0.307
C5 – H14	0.282	−0.976	0.013	−0.328	0.042	−0.286
C7 – H15	0.290	−1.077	0.027	−0.345	0.038	−0.307
N1 – H16	0.348	−1.840	0.057	−0.578	0.059	−0.519
C8 – H17	0.292	−1.085	0.032	−0.343	0.036	−0.307
C8 – H18	0.293	−1.093	0.031	−0.344	0.036	−0.309
C9 – H19	0.286	−0.996	0.031	−0.342	0.046	−0.295
N2 – H23	0.336	−1.852	0.003	−0.538	0.038	−0.501
N2 – H24	0.336	−1.853	0.003	−0.538	0.038	−0.501
N2 – H25	0.336	−1.852	0.003	−0.539	0.038	−0.501
b						
Amphetamine						
Связи				V	G	H
C2 – H11	0.253	−0.751	0.016	−0.265	0.039	−0.226
C3 – H12	0.282	−0.972	0.018	−0.331	0.044	−0.287
C3 – H13	0.280	−0.947	0.020	−0.329	0.046	−0.283
C5 – H16	0.273	−0.911	0.006	−0.321	0.047	−0.274
C5 – H14	0.271	−0.906	0.001	−0.315	0.044	−0.271
C5 – H15	0.272	−0.911	0.004	−0.318	0.045	−0.273
C6 – H17	0.289	−1.017	0.041	−0.348	0.047	−0.301
C7 – H18	0.287	−1.008	0.027	−0.342	0.045	−0.297
N1 – H19	0.327	−1.366	0.076	−0.517	0.088	−0.430
C8 – H20	0.285	−0.995	0.024	−0.340	0.045	−0.294
C9 – H21	0.285	−0.988	0.030	−0.340	0.047	−0.294
C10 – H22	0.284	−0.985	0.033	−0.340	0.047	−0.293
Dopamine						
O2 – H20	0.019	0.090	1.083	−0.022	0.022	0.000
C4 – H12	0.280	−0.954	0.027	−0.332	0.047	−0.285

Table 1.

1	2	3	4	5	6	7
C4 – H13	0.278	−0.934	0.028	−0.329	0.048	−0.281
C6 – H14	0.274	−0.915	0.022	−0.313	0.042	−0.271
C6 – H15	0.260	−0.818	0.024	−0.284	0.040	−0.244
C7 – H16	0.287	−1.002	0.044	−0.345	0.047	−0.298
C8 – H17	0.286	−1.005	0.030	−0.342	0.045	−0.297
C10 – H18	0.284	−0.989	0.025	−0.339	0.046	−0.293
N3 – H19	0.328	−1.379	0.073	−0.520	0.087	−0.432
O1 – H20	0.367	−2.128	0.022	−0.656	0.062	−0.594
O2 – H21	0.369	−2.105	0.023	−0.660	0.067	−0.593
Norepinephrine						
O3 – H22	0.371	−2.131	0.021	−0.666	0.067	−0.599
O2 – H21	0.371	−2.141	0.022	−0.664	0.064	−0.600
N4 – H20	0.338	−1.671	0.036	−0.541	0.061	−0.479
N4 – H19	0.330	−1.747	0.027	−0.531	0.047	−0.484
C8 – H16	0.291	−1.069	0.025	−0.346	0.039	−0.307
C9 – H17	0.285	−0.984	0.045	−0.342	0.048	−0.294
C11 – H18	0.281	−0.958	0.029	−0.334	0.047	−0.287
C7 – H14	0.279	−0.953	0.018	−0.326	0.044	−0.282
C7 – H15	0.276	−0.933	0.018	−0.320	0.044	−0.277
C5 – H13	0.260	−0.814	0.023	−0.277	0.037	−0.240
O1 – H19	0.022	0.100	0.528	−0.025	0.025	0.000
O1 – H16	0.017	0.080	1.566	−0.016	0.018	0.002
O3 – H22	0.371	−2.131	0.021	−0.666	0.067	−0.599
Serotonin						
N3 – H23	0.327	−1.383	0.076	−0.520	0.087	−0.433
C11 – H21	0.284	−0.991	0.023	−0.339	0.046	−0.293
C11 – C13	0.307	−0.775	0.496	−0.414	0.110	−0.304
C13 – H22	0.287	−1.007	0.030	−0.343	0.046	−0.298
C6 – H14	0.280	−0.958	0.015	−0.327	0.044	−0.283
C6 – H15	0.280	−0.948	0.017	−0.329	0.046	−0.283
C8 – H16	0.288	−1.046	0.046	−0.347	0.043	−0.304
N2 – H17	0.349	−1.794	0.064	−0.580	0.066	−0.514
C9 – H18	0.246	−0.721	0.024	−0.257	0.038	−0.218
C9 – H19	0.259	−0.812	0.021	−0.283	0.040	−0.243
C10 – H20	0.284	−0.986	0.034	−0.340	0.047	−0.293
O1 – H24	0.372	−2.127	0.022	−0.664	0.066	−0.598
Tryptamine						
C5 – H13	0.276	−0.930	0.018	−0.326	0.047	−0.279
N2 – H23	0.320	−1.359	0.054	−0.507	0.084	−0.424
H18 – H19	0.009	0.025	0.233	−0.004	0.005	0.001
C10 – H20	0.278	−0.955	0.034	−0.334	0.047	−0.286
C11 – H21	0.280	−0.972	0.031	−0.336	0.047	−0.290
C12 – H22	0.280	−0.971	0.026	−0.336	0.046	−0.289
C5 – H14	0.273	−0.909	0.019	−0.322	0.047	−0.275
C7 – H15	0.285	−1.024	0.064	−0.343	0.044	−0.299
N1 – H16	0.347	−1.826	0.051	−0.570	0.057	−0.513
C8 – H17	0.253	−0.758	0.010	−0.284	0.047	−0.237
C8 – H18	0.244	−0.693	0.014	−0.268	0.047	−0.221
C9 – H19	0.285	−1.033	0.020	−0.340	0.041	−0.299

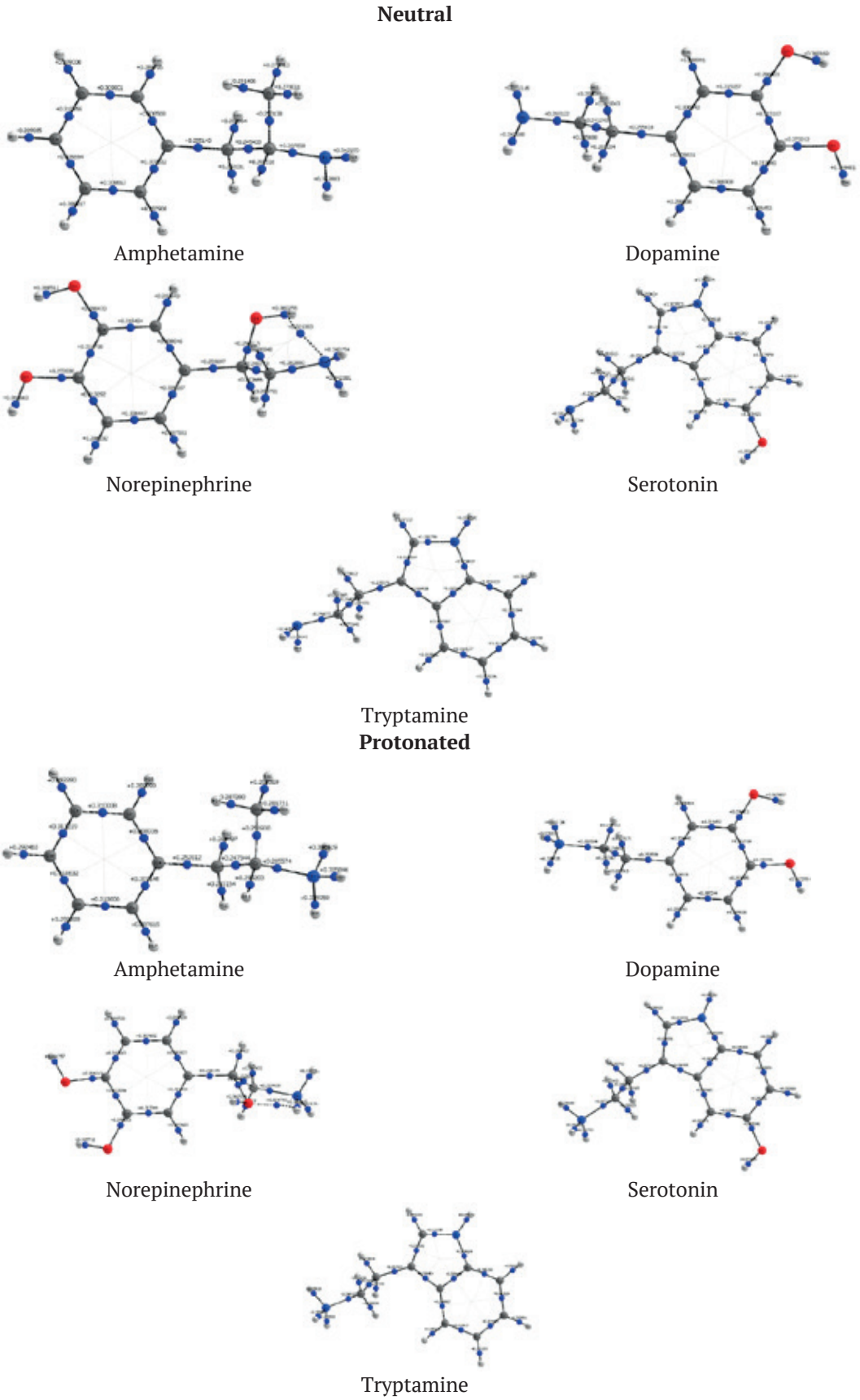

Fig. 2. Electron density of the title compounds

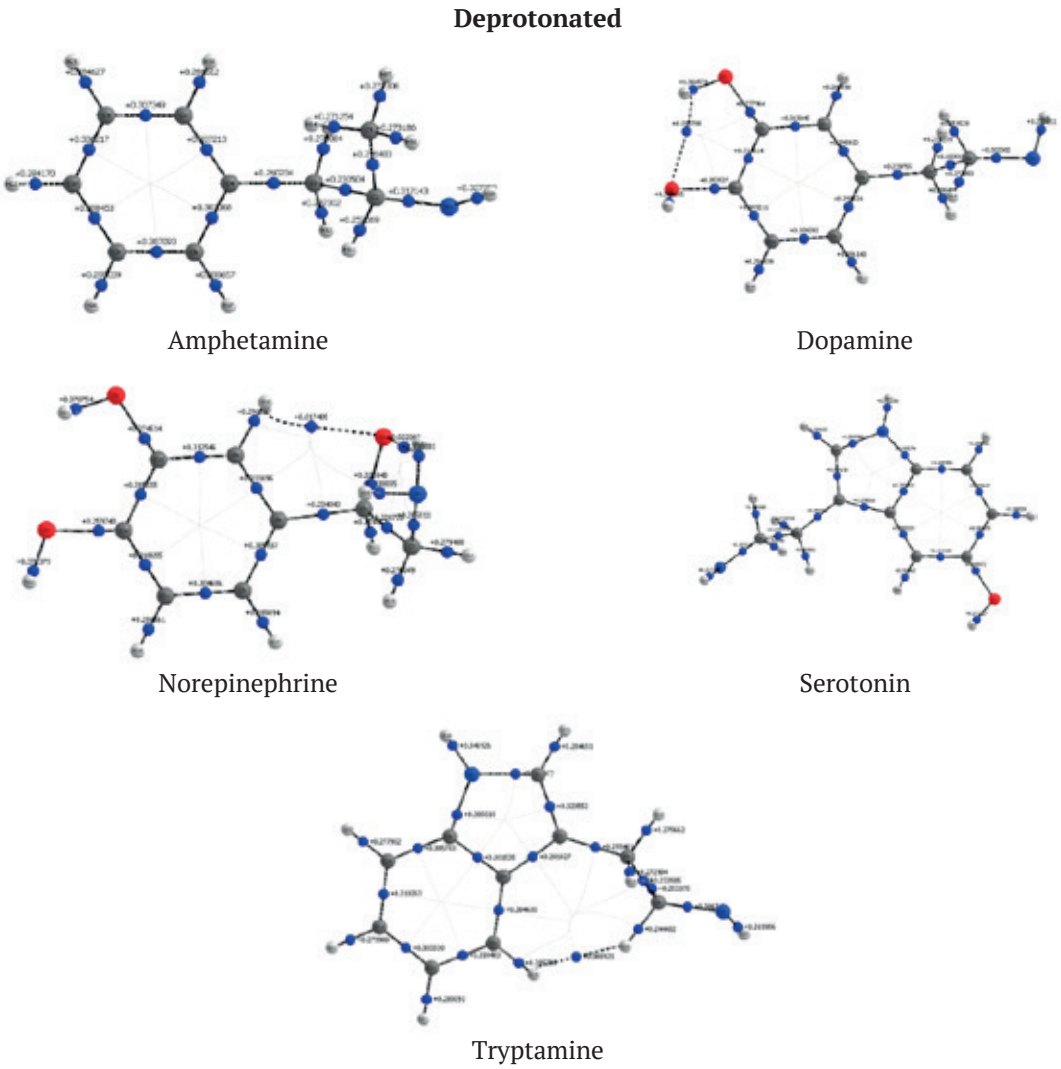

Fig. 2.

weights. Remarkably, all measured values align with the expected ranges for drug-like molecules, highlighting the compounds' suitability for further drug design efforts. In summary, this concise yet informative analysis underscores how a diverse range of physicochemical properties can effectively guide molecular design, ensuring favorable interactions and the potential development of efficacious therapeutic agents.

3.4. Natural Bond Order (NBO) analysis

The investigation included the examination of the Lewis structures of all compounds in their neutral, protonated, and deprotonated forms. This examination was conducted using the B3LYP/6–311+G(d, p) technique and theoretical approaches based on the NBO analysis, as shown in Table 3-7. The NBO analysis is a significant technique used for examining the Lewis structure of a molecule. It offers essential insights into several aspects, including resonance delocalization, bond order, hybridization type, and donor-acceptor interactions. The DFT calculations were used to conduct a comprehensive study, including the entire NBO analysis and the analysis of the second-order Fock matrix perturbation theory. As well as, the second order energy predicts the stabilization energy, which represents the strength of the delocalization interactions, for each donor NBO (i), acceptor NBO (j), and the $E(2)$ associated with the electron delocalization between the donor and the acceptor [36-40].

In the above equation, the symbol "qi" represents the occupancy of the donor orbital, while "εi" and "εj" denote the diagonal elements. "$F(i,j)$" represents the off-diagonal NBO Fock matrix element. A greater value of $E(2)$ signifies

Table 2. Physiochemical property values of study compounds and standard drug molecules

Descriptors	Amphetamine	Dopamine	Norepinephrine	Serotonin	Tryptamine	Expected range
Hydrogen bond donor (HBD)	1	3	4	2	2	< 5
Hydrogen bond acceptors (HBA)	1	3	4	2	1	< 10
Polar surface area (PSA)	26.02	66.48	86.71	62.04	41.81	< 140
Molecular weight	135.21	153.18	169.18	176.22	160.22	< 500
Number of rotatable bonds	2	2	2	2	2	< 10
Molar refractivity	43.73	42.97	44.13	52.80	50.78	40–160
	Protonated					
Hydrogen bond donor (HBD)	1	3	4	3	2	< 5
Hydrogen bond acceptors (HBA)	0	2	3	1	0	< 10
Polar surface area (PSA)	3.24	43.70	63.93	39.26	19.03	< 140
Molecular weight	136.21	154.19	170.19	177.22	161.22	< 500
Number of rotatable bonds	2	2	2	2	2	< 10
Molar refractivity	44.69	43.93	45.09	53.13	51.74	40–160
	Deprotonated					
Hydrogen bond donor (HBD)	1	3	4	3	2	< 5
Hydrogen bond acceptors (HBA)	1	3	4	2	1	< 10
Polar surface area (PSA)	26.02	64.31	171.19	62.04	41.81	< 140
Molecular weight	137.22	153.18	86.71	178.23	160.22	< 500
Number of rotatable bonds	2	0	2	2	2	< 10
Molar refractivity	43.73	45.97	44.13	52.80	50.78	40–160

an increased level of interaction between electron donors and electron acceptors.

In this work, the NBO analysis reveals that the highest lone pair of electrons on oxygen (N2) inside the carboxylic group undergoes delocalization towards the π* antibonding molecular orbital of the C4-C8 bond within the same carboxylic group for protonated serotonin compounds. This delocalization process results in a significant stabilization energy of 42.97 kcal/mol, as seen in Table 1.

The delocalization interaction π*(C 11 – C 13) to π*(C 5 – C 7) in protonated serotonin is of significant importance, with a stabilization energy of 261.16 kcal/mol. Similarly, with the neutral norepinephrine molecule, the interaction between π*(C 11 – C 12) and π*(C 8 – C 10) is noteworthy, with a stabilization energy of 256.38 kcal/mol. The findings show that σ→σ* interactions have a lower delocalization energy compared to π→π* interactions. The electron density attributed to σ bonds exhibits greater magnitude when compared to that of π bonds.

3.5. Nonlinear optical properties (NLO)

Nonlinear optical (NLO) materials are of significant importance in nonlinear optics, particularly because of their significant effect on information technology and industrial applications. The first static analysis was performed on the geometry that has undergone optimization using the B3LYP/6-311G++(d,p) method. The initial static hyperpolarizability, represented as: is a tensor of three dimensions with a rank of three, which may be mathematically represented by a 3×3×3 matrix. The total static dipole moment mean polarizability , and initial static hyperpolarizability may be determined by using the equations that include the x, y, and z component [38, 41].

A high value of a particular component of the polarizability and hyperpolarizability indices indicates that there has been a considerable delocalization of charge in one or more specific directions [42, 43]. The total molecular dipole moment , mean polarizability, and first hyperpolarizability of the title have been calculated and are presented in Table 8.

Table 3. Second-order Perturbation Theory Analysis of Fock Matrix in NBO for Amphetamine

Donor NBO (*i*)	Acceptor NBO (*j*)	*E*(2), kcal/mol	*E*(*j*)-*E*(*i*), a.u.	*F*(*i*,*j*), a.u.
Neutral				
πC 4 – C 7	π* C 6 – C 8	19.64	0.28	0.066
πC 4 – C 7	π* C 9 – C 10	21.47	0.28	0.069
πC 6 – C 8	π* C 4 – C 7	20.68	0.29	0.069
πC 6 – C 8	π* C 9 – C 10	19.62	0.28	0.067
σC 6 – H 17	σ*C 4 – C 7	3.95	1.1	0.059
σC 7 – H 18	σ* C 4 – C 6	4.01	1.09	0.059
σC 7 – H 18	σ*C 9 – C 10	3.53	1.1	0.056
πC 9 – C 10	π* C 4 – C 7	19.38	0.29	0.067
πC 9 – C 10	π* C 6 – C 8	20.76	0.28	0.068
σC 9 – H 22	σ* C 4 – C 7	3.79	1.1	0.058
Protonated				
πC 4 – C 7	π* C 6 – C 8	19.23	0.29	0.067
πC 4 – C 7	π* C 9 – C 10	18.18	0.3	0.066
σ C 5 – H 14	σ*N 1 – C 2	5.68	0.68	0.056
π C 6 – C 8	π* C 4 – C 7	21.44	0.27	0.069
π C 6 – C 8	π* C 9 – C 10	18.87	0.29	0.067
σ C 6 – H 17	σ* C 4 – C 7	4.11	1.1	0.06
σ C 7 – H 18	σ* C 4 – C 6	4.17	1.09	0.06
π C 9 – C 10	π* C 4 – C 7	22.53	0.27	0.069
π C 9 – C 10	π* C 6 – C 8	20.99	0.27	0.069
π*C 4 – C 7	π*C 9 – C 10	171.97	0.02	0.082
Deprotonated				
π C 4 – C 6	π*C 7 – C 9	20.47	0.26	0.066
π C 4 – C 6	π*C 8 – C 10	26.03	0.25	0.073
π C 7 – C 9	π*C 4 – C 6	18.9	0.3	0.068
π C 7 – C 9	π*C 8 – C 10	18.96	0.28	0.066
π C 8 – C 10	π*C 4 – C 6	15.76	0.3	0.063
π C 8 – C 10	π*C 7 – C 9	19.11	0.29	0.067
σC 9 – H 21	σ*C 4 – C 7	3.65	1.12	0.057
LP (2) N 1	σ* C 2 – H 11	20.35	0.48	0.092
π*C 7 – C 9	π*C 4 – C 6	196.57	0.02	0.084
π*C 8 – C 10	π*C 4 – C 6	133.51	0.02	0.08

Table 4. Second Order Perturbation Theory Analysis of Fock Matrix in NBO for dopamine

Donor NBO (i)	Acceptor NBO (j)	E(2), kcal/mol	E(j)-E(i), a.u.	F(i,j), a.u.
1	2	3	4	5
Neutral				
σ O 1 – H 21	σ*C 7 – C 9	5.47	1.31	0.076
π C 5 – C 8	π* C 7 – C 9	18.23	0.28	0.064
π C 5 – C 8	π* C 10 – C 11	20.8	0.27	0.068
π C 7 – C 9	π* C 5 – C 8	20.73	0.3	0.071
π C 7 – C 9	π* C 10 – C 11	19.68	0.28	0.068
σ C 8 – C 10	σ* O 2 – C 11	5.08	1.02	0.064
π C 10 – C 11	π* C 5 – C 8	17.09	0.31	0.066
π C 10 – C 11	π* C 7 – C 9	18.6	0.3	0.068

Table 4.

1	2	3	4	5
LP (2) O 1	π* C 7 – C 9	28.74	0.35	0.095
π* C 10 – C 11	π* C 5 – C 8	179.74	0.02	0.08
Protonated				
σ O 1 – H 21	σ*C 7 – C 9	5.64	1.3	0.077
σ O 2 – H 22	σ* C 9 – C 11	4.29	1.27	0.067
π C 5 – C 8	π* C 7 – C 9	17.38	0.29	0.065
π C 5 – C 8	π* C 10 – C 11	17.4	0.29	0.065
π C 7 – C 9	π* C 5 – C 8	20.91	0.29	0.07
π C 7 – C 9	π* C 10 – C 11	18.74	0.29	0.066
σ C 8 – C 10	σ* O 2 – C 11	4.88	1.05	0.064
π C 10 – C 11	π* C 5 – C 8	19.58	0.29	0.069
πC 10 – C 11	π* C 7 – C 9	18.85	0.29	0.067
LP (2) O 1	π* C 7 – C 9	32.29	0.33	0.098
Deprotonated				
σ N 3 – H 19	σ* C 6 – H 14	5.9	0.94	0.067
σ C 4 – C 6	σ* C 5 – C 7	7.11	0.47	0.057
π C 5 – C 7	π* C 8 – C 10	18.2	0.26	0.061
π C 5 – C 7	π* C 9 – C 11	30.11	0.24	0.079
π C 8 – C 10	π* C 5 – C 7	17.25	0.3	0.067
π C 8 – C 10	π*C 9 – C 11	16.07	0.27	0.063
π C 9 – C 11	π*C 8 – C 10	21.98	0.3	0.073
LP (2) O 1	π*C 9 – C 11	26.91	0.35	0.095
π* C 8 – C 10	π* C 5 – C 7	227.99	0.01	0.082
π*C 9 – C 11	π* C 8 – C 10	254.9	0.01	0.079

Table 5. Second Order Perturbation Theory Analysis of Fock Matrix in NBO for Norepinephrine

Donor NBO (*i*)	Acceptor NBO (*j*)	*E*(2), kcal/mol	*E*(*j*)-*E*(*i*), a.u.	*F*(*i*,*j*), a.u.
1	2	3	4	5
Neutral				
σ O 2 – H 22	σ* C 8 – C 10	5.43	1.31	0.076
π C 6 – C 9	π* C 8 – C 10	18.14	0.28	0.065
π C 6 – C 9	π*C 11 – C 12	20.41	0.27	0.068
π C 8 – C 10	π*C 6 – C 9	21.08	0.29	0.071
π C 8 – C 10	π* C 11 – C 12	20.66	0.28	0.069
σ C 9 – C 11	σ* O 3 – C 12	5.03	1.02	0.064
π C 11 – C 12	π* C 8 – C 10	17.97	0.3	0.067
LP (2) O 2	π*C 8 – C 10	28.2	0.35	0.094
π* C 11 – C 12	π* C 6 – C 9	179.59	0.02	0.08
π*C 11 – C 12	π*C 8 – C 10	256.38	0.01	0.083
Protonated				
σ O 2 – H 22	σ* C 8 – C 10	5.66	1.3	0.077
π C 6 – C 9	π* C 8 – C 10	17.55	0.29	0.065
π C 6 – C 9	π*C 11 – C 12	16.78	0.29	0.063
π C 8 – C 10	π* C 6 – C 9	20.33	0.28	0.069
π C 8 – C 10	π* C 11 – C 12	18.85	0.29	0.066
σ C 9 – H 17	σ* C 6 – C 8	4.34	1.09	0.061
π C 11 – C 12	π* C 6 – C 9	20.31	0.29	0.07
π C 11 – C 12	π* C 8 – C 10	18.53	0.29	0.066
LP (2) O 2	π* C 8 – C 10	32.64	0.33	0.098
LP (2) O 3	π* C 11 – C 12	28.84	0.35	0.096

Table 5.

1	2	3	4	5
Deprotonated				
σ O 2 – H 21	σ* C 8 – C 10	5.17	1.34	0.074
π C 8 – C 10	π* C 6 – C 9	20.78	0.3	0.071
π C 8 – C 10	π*C 11 – C 12	22.32	0.26	0.07
σ C 9 – C 11	σ* O 3 – C 12	5.13	0.99	0.064
LP (2) O 1	σ* C 5 – C 6	19.19	0.55	0.093
LP (3) O 1	σ*C 5 – H 13	16.01	0.56	0.086
LP (1) O 2	σ* C 10 – C 12	5.71	1.15	0.073
LP (2) O 2	π* C 8 – C 10	23.94	0.37	0.09
π* C 8 – C 10	π* C 6 – C 9	212.92	0.02	0.085
π* C 11 – C 12	π* C 8 – C 10	131.19	0.03	0.083

Table 6. Second-order Perturbation Theory Analysis of Fock Matrix in NBO for Serotonin

Donor NBO (*i*)	Acceptor NBO (*j*)	*E*(2), kcal/mol	*E*(*j*)-*E*(*i*), a.u.	*F*(*i*,*j*), a.u.
Neutral				
σ C 4 – C 8	σ* C 5 – C 10	5.02	1.27	0.071
π C 4 – C 8	π* C 5 – C 7	16.32	0.29	0.068
π C 5 – C 7	π* C 4 – C 8	18.11	0.28	0.065
π C 5 – C 7	π* C 10 – C 12	17.78	0.27	0.063
π C 5 – C 7	π*C 11 – C 13	21.14	0.27	0.069
π C 10 – C 12	π*C 5 – C 7	18.2	0.29	0.069
π C 10 – C 12	π* C 11 – C 13	16.1	0.29	0.062
σ C 11 – C 13	σ* N 2 – C 7	6.15	1.16	0.075
π C 11 – C 13	π* C 10 – C 12	19.25	0.29	0.069
LP (1) N 2	π* C 4 – C 8	35.4	0.3	0.093
Protonated				
σ C 5 – C 7	σ* C 4 – C 6	5.29	1.06	0.067
π C 5 – C 7	π*C 4 – C 8	19.79	0.26	0.064
π C 10 – C 12	π*C 5 – C 7	19.4	0.29	0.071
π C 10 – C 12	π* C 11 – C 13	14.93	0.3	0.06
σ C 11 – C 13	σ* N 2 – C 7	6.27	1.15	0.076
π C 11 – C 13	π* C 10 – C 12	20.35	0.28	0.069
LP (2) O 1	π*C 10 – C 12	31.11	0.34	0.098
LP (1) N 2	π* C 4 – C 8	42.97	0.28	0.099
π* C 5 – C 7	π* C 11 – C 13	233.04	0.01	0.082
π* C 10 – C 12	π*C 11 – C 13	254.27	0.01	0.082
Deprotonated				
σ C 4 – C 8	σ* C 5 – C 10	5.29	1.25	0.073
πC 5 – C 7	π*C 4 – C 8	17.65	0.29	0.066
πC 5 – C 7	π*C 10 – C 12	18.89	0.26	0.063
πC 5 – C 7	π*C 11 – C 13	24.39	0.25	0.07
σC 6 – H 15	σ* C 4 – C 8	5.06	1.05	0.065
πC 10 – C 12	π*C 11 – C 13	16.24	0.28	0.063
πC 11 – C 13	π*C 10 – C 12	19.18	0.29	0.069
LP (1) N 2	π*C 5 – C 7	31.23	0.3	0.091
π*C 5 – C 7	π*C 4 – C 8	111.28	0.02	0.067
π*C 11 – C 13	π*C 5 – C 7	261.16	0.02	0.083

Table 7. Second-order Perturbation Theory Analysis of Fock Matrix in NBO for Tryptamine

Donor NBO (*i*)	Acceptor NBO (*j*)	*E*(2), kcal/mol	*E*(*j*)-*E*(*i*), a.u.	*F*(*i*,*j*), a.u.
Neutral				
s C 4 – C 6	s* C 3 – C 5	4.43	1.1	0.063
p C 4 – C 6	p* C 3 – C 7	18.35	0.28	0.065
p C 4 – C 6	p* C 9 – C 11	19.82	0.28	0.068
p C 4 – C 6	p* C 10 – C 12	19.01	0.27	0.065
s C 5 – H 13	s* C 3 – C 4	4.86	1.02	0.063
p C 9 – C 11	p* C 4 – C 6	16.63	0.28	0.065
p C 9 – C 11	p* C 10 – C 12	19.45	0.28	0.067
p C 10 – C 12	p* C 4 – C 6	18.9	0.28	0.069
p C 10 – C 12	p* C 9 – C 11	17.12	0.29	0.064
LP (1) N 1	p* C 4 – C 6	35.26	0.3	0.094
Protonated				
s C 4 – C 6	s*C 3 – C 5	5.16	1.06	0.066
p C 4 – C 6	p* C 3 – C 7	19.81	0.26	0.065
p C 4 – C 6	p* C 9 – C 11	18.58	0.28	0.066
p C 9 – C 11	p* C 10 – C 12	18.24	0.29	0.066
s C 10 – C 12	s* N 1 – C 6	6.36	1.14	0.076
p C 10 – C 12	p* C 4 – C 6	20.46	0.27	0.07
p C 10 – C 12	p* C 9 – C 11	18.7	0.28	0.065
LP (1) N 1	p* C 3 – C 7	41.22	0.28	0.098
p* C 4 – C 6	p* C 9 – C 11	249.47	0.01	0.079
p* C 4 – C 6	p* C 10 – C 12	207.04	0.02	0.081
Deprotonated				
p C 3 – C 7	p* C 4 – C 9	13.95	0.31	0.061
p C 4 – C 9	p* C 3 – C 7	10.81	0.31	0.052
p C 4 – C 9	p* C 6 – C 10	13.27	0.3	0.057
p C 4 – C 9	p* C 11 – C 12	12.49	0.28	0.053
p C 6 – C 10	p* C 11 – C 12	11.52	0.3	0.053
p C 11 – C 12	p* C 6 – C 10	8.44	0.31	0.047
LP (1) N 1	p* C 6 – C 10	16.18	0.38	0.072
LP (2) N 2	s* C 8 – H 18	9.75	0.6	0.072
p* C 6 – C 10	p* C 4 – C 9	115.66	0.02	0.073
p* C 11 – C 12	p* C 6 – C 10	85.65	0.01	0.061

The polarizabilities and the hyperpolarizabilities that were acquired from the GAUSSIAN 09 output were initially represented in atomic units (a.u.). These computed values have been translated into electrostatic units (e.s.u.forof making comparisons and interpretations more straightforward. For polarizabilities, 1 a.u. is equal to $0.1482 \cdot 10^{-24}$ e.s.u., and for hyperpolarizabilities, 1 a.u. is equal to $8.6393 \cdot 10^{-33}$ e.s.u.

As observed in Table 8, the computed dipole moment values for the compounds under investigation, both in their protonated and deprotonated states, are higher than the dipole moment of urea, which is equal to 1.3732 D. When exploring the nonlinear optical (NLO) features of molecular systems, urea is often used as a model molecule because of its well-characterized nonlinear optical behavior. Because of this, it has often been used as a benchmark in many comparative studies.

The polarizability values were calculated for all compounds in their neutral, protonated, and deprotonated states. These values are reported in Table 8. The findings show that the polarizability is reduced in the deprotonated state as compared with the corresponding protonated and neutral states.

Table 8. NLO parameters for all compounds

Parameters	Neutral	Protonated	Deprotonated	Neutral	Protonated	Deprotonated
1	2	3	4	5	6	7
	Amphetamine			Dopamine		
μ_t	1.26	11.90	9.25	2.86	14.82	12.42
α_{xx}	−57.96	−2.26	−106.59	−58.06	30.59	−131.00
α_{yy}	−56.53	−50.44	−65.72	−60.58	−55.79	−70.20
α_{zz}	−62.99	57.11	−69.70	−68.66	−62.17	−70.06
α_t	−59.16	1.47	−80.67	−62.43	−29.13	−90.42
$\alpha(esu)*10^{-24}$	−8.77	0.22	−11.96	−9.25	−4.32	−13.40
β_{xxx}	0.97	165.11	−121.75	76.32	−293.07	−314.64
β_{xyy}	3.67	11.87	11.87	7.37	−0.96	−4.65
β_{xzz}	7.24	22.15	−5.74	10.86	−16.95	−31.93
β_x	11.88	199.13	−115.62	94.54	−310.98	−351.22
β_{yyy}	−4.21	−5.31	0.89	−9.86	−8.35	−6.61
β_{xxy}	−13.78	−19.99	20.46	−21.18	6.97	10.76
β_{yzz}	−0.83	0.11	0.13	2.91	5.32	0.49
β_y	−18.83	−25.19	21.48	−28.13	3.94	4.65
β_{zzz}	0.34	0.85	−1.72	−2.77	−9.10	7.08
β_{xxz}	21.92	2.49	30.89	28.10	−38.04	−25.57
β_{yyz}	−2.49	−1.12	−2.19	−2.62	−3.70	1.97
β_z	19.76	2.22	26.99	22.71	−50.84	−16.52
$\beta_0(esu)*10^{-33}$	29.77	200.73	120.66	101.22	315.13	351.64
	Norepinephrine			Serotonin		
μ_t	4.37	11.51	10.82	1.10	16.41	12.51
α_{xx}	−48.16	11.56	−102.27	−84.18	−1.57	−155.02
α_{yy}	−68.01	−61.36	−78.14	−56.30	−44.08	−74.40
α_{zz}	−72.25	−62.33	−82.33	−78.32	−74.52	−83.09
α_t	−62.80	−37.38	−87.58	−72.93	−40.06	−104.17
$\alpha(esu)*10^{-24}$	−9.31	−5.54	−12.98	−10.81	−5.94	−15.44
β_{xxx}	1.81	188.37	−141.20	27.98	−311.06	264.60
β_{xyy}	−9.96	−1.25	−23.60	−12.03	−37.53	38.08
β_{xzz}	6.77	27.16	−32.30	−9.79	−21.39	4.74
β_x	−1.39	214.28	−197.10	6.17	−369.98	307.42
β_{yyy}	−7.85	6.67	−7.18	4.00	−6.17	15.89
β_{xxy}	−33.69	7.75	−29.43	5.65	−75.10	98.86
β_{yzz}	3.40	−8.23	3.11	−8.20	−12.22	−3.66
β_y	−38.14	6.19	−33.50	1.45	−93.49	111.10
β_{zzz}	9.01	7.39	0.64	2.28	5.37	−0.97
β_{xxz}	23.32	−54.05	−10.11	18.24	28.03	3.51

Table 8.

1	2	3	4	5	6	7
β_{yyz}	0.43	−2.69	7.69	−0.58	0.87	3.37
β_z	32.77	−49.35	−1.78	19.94	34.28	5.92
$\beta_0\,(esu)*10^{-33}$	50.34	219.98	199.93	20.92	383.15	326.93
			Tryptamine			
μ_t	1.35	14.48	11.70			
α_{xx}	−70.12	10.12	−134.08			
α_{yy}	−57.78	−49.61	−76.20			
α_{zz}	−73.26	−69.73	−77.43			
α_t	−67.05	−36.41	−95.90			
$\alpha(esu)*10^{-24}$	−9.94	−5.40	−14.21			
β_{xxx}	30.27	−285.98	−231.75			
β_{xyy}	−0.31	−11.74	−20.72			
β_{xzz}	−15.30	−26.16	1.77			
β_x	14.67	−323.88	−250.69			
β_{yyy}	24.41	19.17	14.72			
β_{xxy}	−16.25	−52.43	67.38			
β_{yzz}	−0.27	−2.65	3.40			
β_y	7.88	−35.92	85.50			
β_{zzz}	3.01	5.81	−0.35			
β_{xxz}	17.98	28.07	−9.63			
β_{yyz}	1.67	3.63	−8.61			
β_z	22.67	37.51	−18.59			
$\beta_0\,(esu)*10^{-33}$	−70.12	10.12	−134.08			

The determination of the size has significant importance within the context of a nonlinear optical (NLO) system. The values of the deprotonated dopamine and protonated serotonin molecules are found to be relatively greater than urea. Specifically, the β value of urea is measured to be $343.272{\cdot}10^{-33}$ esu, but other findings show that the initial hyperpolarizability value is less than the hyperpolarizability value of urea. The findings show that deprotonated dopamine and protonated serotonin have promise for uses in Nonlinear Optical (NLO) systems.

3.6. Quantum chemical parameters and Molecular orbitals (MOs)

Table 9 presents a detailed overview of the quantum chemical parameters for Amphetamine, Dopamine, Norepinephrine, Serotonin, and Tryptamine, in their neutral, protonated, and deprotonated states. These parameters provide valuable insights into the compounds' electronic properties, reactivity, and stability, all of which are crucial considerations in evaluating their potential as drug candidates [44, 45].

Examining the Highest Occupied Molecular Orbital (HOMO) and Lowest Unoccupied Molecular Orbital (LUMO) energies reveals important details about the compounds' ionization potential and electron affinity [46]. For example, Amphetamine's neutral state shows a HOMO energy of −6.304 eV, showing its ability to donate electrons, while its LUMO energy of 0.049 eV suggests a lower tendency to accept electrons. Similar trends are observed across the compounds, with Tryptamine displaying a comparable pattern.

The energy gap, representing the difference between HOMO and LUMO energies, reflects the compounds' stability and their capacity

Table 9. Quantum chemical parameters for title compounds

Parameters	Neutral	Protonated	Deprotonated
1	2	3	4
Amphetamine			
HOMO, (eV)	−6.304	−9.798	1.868
LUMO, (eV)	0.049	−4.235	3.585
Ionization energy, (eV)	6.304	9.798	−1.868
Electron Affinity, (eV)	−0.049	4.235	−3.585
Energy gap, (eV)	6.353	5.563	1.717
Hardness, (eV)	3.177	2.782	0.859
Softness, $(eV)^{-1}$	0.157	0.180	0.582
Electronegativity, (eV)	3.128	7.017	−2.727
Chemical potential, (eV)	−3.128	−7.017	2.727
Electrophilicity, (eV)	1.540	8.850	4.330
Nucleophilicity, $(eV)^{-1}$	0.650	0.113	0.231
Back-donation, (eV)	−0.794	−0.695	−0.215
Electron transfer	0.985	2.523	−3.176
Total energy T.E., (a.u)	−405.559	−405.936	−404.895
Dopamine			
HOMO, (eV)	−5.522	1.492	1.492
LUMO, (eV)	0.173	3.653	3.653
Ionization energy, (eV)	5.522	−1.492	−1.492
Electron Affinity, (eV)	−0.173	−3.653	−3.653
Energy gap, (eV)	5.695	2.161	2.161
Hardness, (eV)	2.848	1.081	1.081
Softness, $(eV)^{-1}$	0.176	0.463	0.463
Electronegativity, (eV)	2.675	−2.573	−2.573
Chemical potential, (eV)	−2.675	2.573	2.573
Electrophilicity, (eV)	1.256	3.062	3.062
Nucleophilicity, $(eV)^{-1}$	0.796	0.327	0.327
Back-donation, (eV)	−0.712	−0.270	−0.270
Electron transfer	0.939	−2.381	−2.381
Total energy T.E., (a.u)	−516.681	−515.018	−515.017
Norepinephrine			
HOMO, (eV)	−5.45	−8.761	0.25
LUMO, (eV)	−0.313	−3.903	3.972
Ionization energy, (eV)	5.450	8.761	−0.250
Electron Affinity, (eV)	0.313	3.903	−3.972
Energy gap, (eV)	5.137	4.858	3.722
Hardness, (eV)	2.569	2.429	1.861
Softness, $(eV)^{-1}$	0.195	0.206	0.269
Electronegativity, (eV)	2.882	6.332	−2.111
Chemical potential, (eV)	−2.882	−6.332	2.111
Electrophilicity, (eV)	1.616	8.253	1.197
Nucleophilicity, $(eV)^{-1}$	0.619	0.121	0.835
Back-donation, (eV)	−0.642	−0.607	−0.465
Electron transfer	1.122	2.607	−1.134
Total energy T.E., (a.u)	−591.899	−592.282	−591.286
Serotonin			
HOMO, (eV)	−5.184	−8.095	1.902
LUMO, (eV)	−0.125	−4.355	3.005
Ionization energy, (eV)	5.184	8.095	−1.902

Table 9.

1	2	3	4
Electron Affinity, (eV)	0.125	4.355	−3.005
Energy gap, (eV)	5.059	3.740	1.103
Hardness, (eV)	2.530	1.870	0.552
Softness, $(eV)^{-1}$	0.198	0.267	0.907
Electronegativity, (eV)	2.655	6.225	−2.454
Chemical potential, (eV)	−2.655	−6.225	2.454
Electrophilicity, (eV)	1.393	10.361	5.458
Nucleophilicity, $(eV)^{-1}$	0.718	0.097	0.183
Back-donation, (eV)	−0.632	−0.468	−0.138
Electron transfer	1.049	3.329	−4.449
Total energy T.E., (a.u)	−573.030	−573.460	−572.361
Tryptamine			
HOMO, (eV)	−5.284	−8.41	2.122
LUMO, (eV)	−0.086	−4.343	3.14
Ionization energy, (eV)	5.284	8.410	−2.122
Electron Affinity, (eV)	0.086	4.343	−3.140
Energy gap, (eV)	5.198	4.067	1.018
Hardness, (eV)	2.599	2.034	0.509
Softness, $(eV)^{-1}$	0.192	0.246	0.982
Electronegativity, (eV)	2.685	6.377	−2.631
Chemical potential, (eV)	−2.685	−6.377	2.631
Electrophilicity, (eV)	1.387	9.997	6.800
Nucleophilicity, $(eV)^{-1}$	0.721	0.100	0.147
Back-donation, (eV)	−0.650	−0.508	−0.127
Electron transfer	1.033	3.136	−5.169
Total energy T.E., (a.u)	−497.713	−498.190	−497.140

for electronic transitions [47]. Importantly, all compounds exhibit energy gap values that fall within the expected range, underscoring their potential stability and reactivity. For instance, Norepinephrine's neutral state boasts an energy gap of 5.137 eV, highlighting its suitability for electronic transitions and reactivity.

Regarding hardness, a measure of resistance to electron addition or removal, values range from 0.509 eV (Tryptamine) to 3.177 eV (Amphetamine). These values signify the compounds' ability to maintain stability during chemical interactions. Electronegativity, indicative of electron-attracting ability, provides insights into polarity and reactivity [48, 49]. Dopamine's electronegativity of 2.675 eV aligns with expectations and underscores its balanced electron-attracting behavior.

Comparing the compounds' parameter values to the expected ranges underscores their suitability for drug design. Ionization energy values within the expected ranges show their readiness for electron donation and participation in chemical reactions. Similarly, electron transfer energies suggest their potential for electron donation or acceptance during reactions, with Amphetamine displaying a value of 0.985 in its neutral state.

Molecular Orbitals (MOs) (Fig. 3–7), particularly HOMO and LUMO, are pivotal for understanding electronic structure and reactivity. In Gaussian software, these MOs can be visualized by using different signs and colours to denote the wave function and the electron density of the orbital. The HOMO depicts regions of high electron density, where electrons are prone to be donated or transferred, implying nucleophilic reactivity. The LUMO depicts regions of low electron density, where electrons are prone to be accepted or received, implying electrophilic reactivity [50-53]. Protonation and deprotonation are processes where a molecule gains or loses a proton (H+), respectively. This alters the charge, shape, and reactivity of the molecule, as well

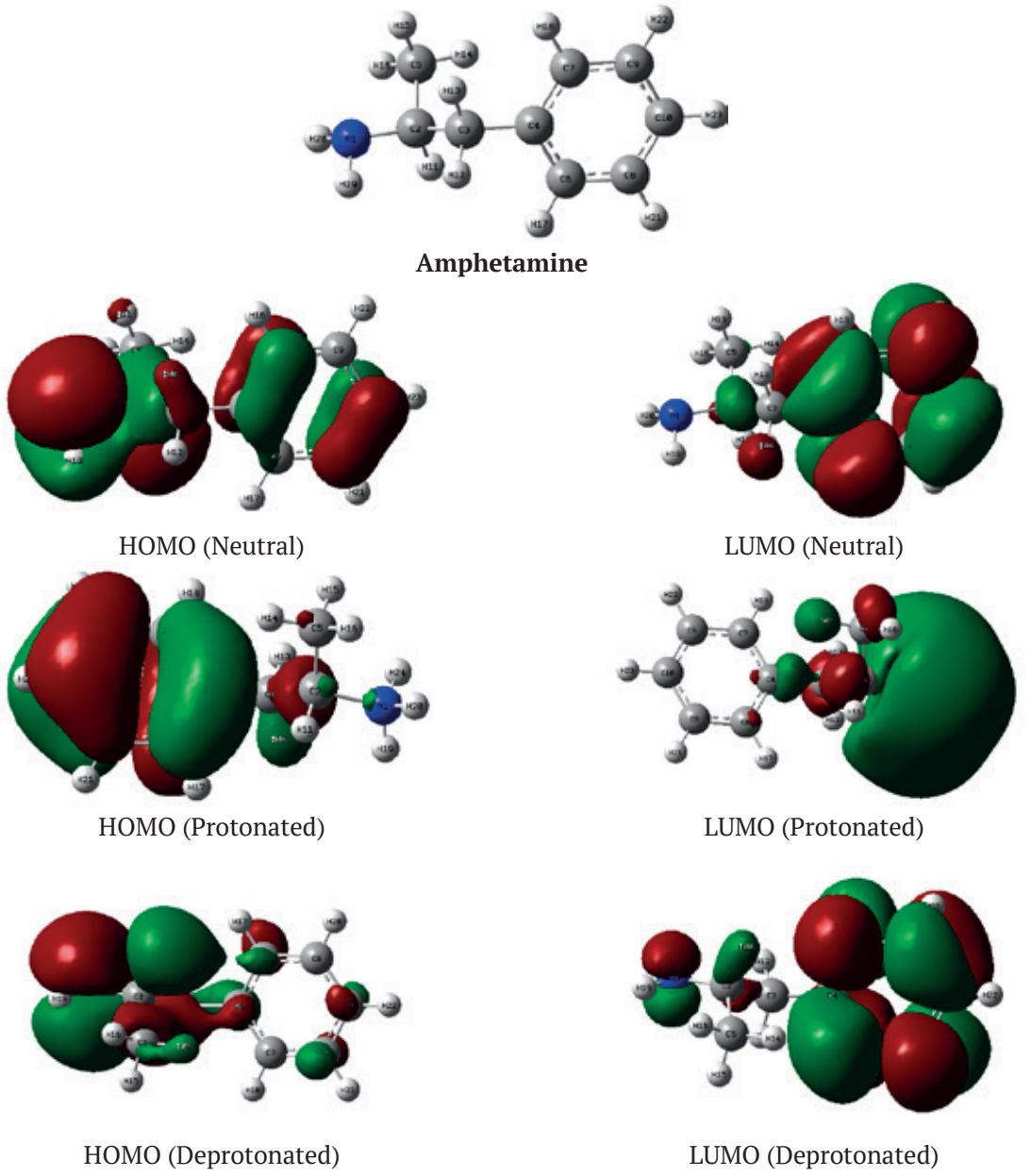

Fig. 3. Optimized structures, HOMO, and LUMO energies for Neutral, protonated, deprotonated

as the MOs, which are the regions where the electrons are distributed in the molecule.

For example, the quantum chemical parameters in Table 9 reveal the impact of protonation and deprotonation on amphetamine's electronic properties. Protonation causes the HOMO to shift to lower energy levels (from –6.304 to –9.798 eV) and the LUMO to lower energy levels (from 0.049 to –4.235 eV), leading to a reduced energy gap (from 6.353 to 5.563 eV). In contrast, deprotonation shifts the HOMO to higher energy levels (from -6.304 to 1.868 eV) and the LUMO to higher energy levels (from 0.049 to 3.585 eV), resulting in a narrower energy gap (from 6.353 to 1.717 eV). These changes highlight how protonation and deprotonation influence amphetamine's reactivity and electron-donating or -accepting properties, Similar patterns of energy shifts are observed for Dopamine, Norepinephrine, Serotonin, and Tryptamine.

Also, In the Fig. 3, you can see how protonation and deprotonation modify the shape and size of

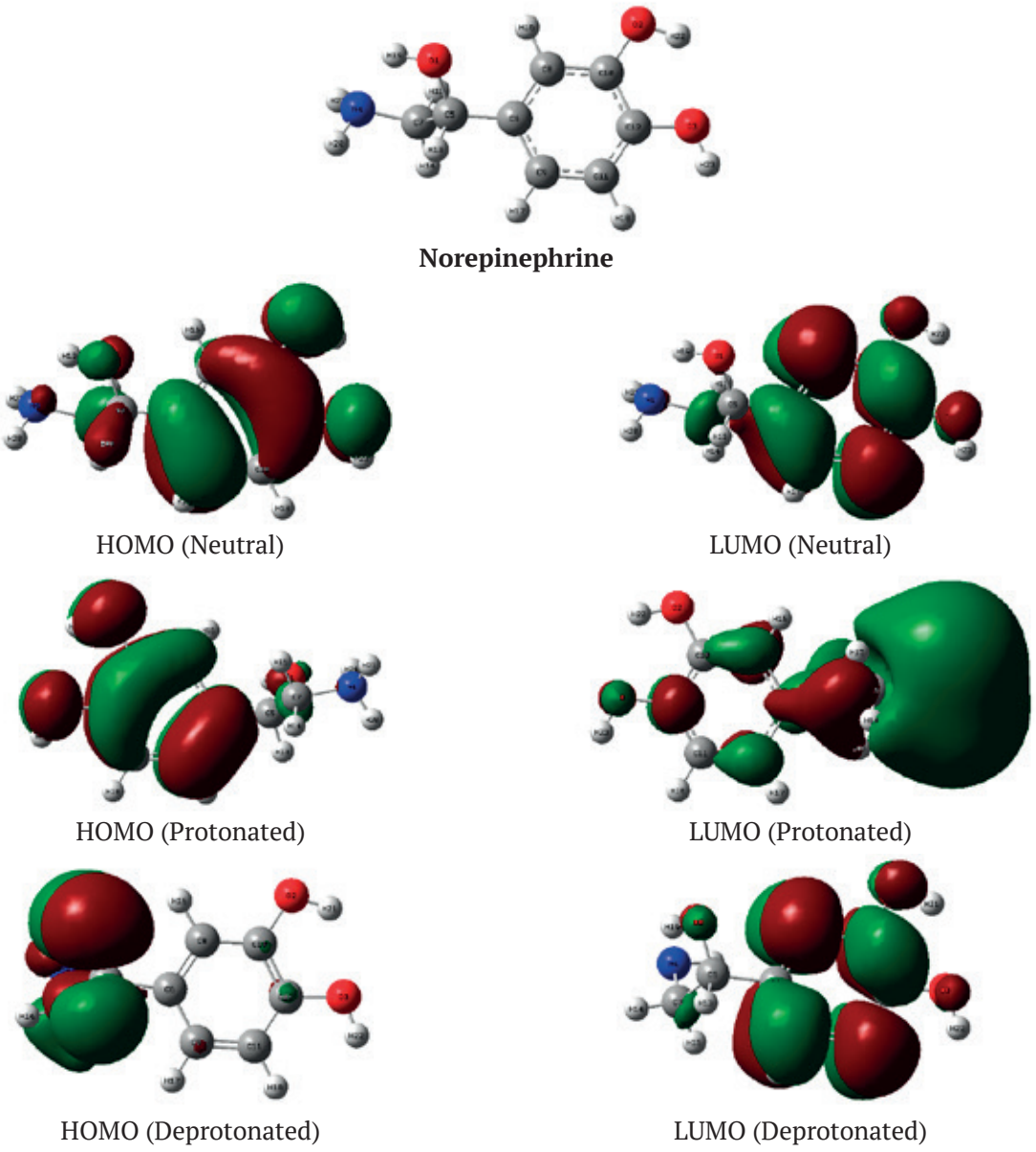

Fig. 4. Optimized structures, HOMO, and LUMO energies for Neutral, -protonated, and deprotonated

the lobs in the HOMO and LUMO of amphetamine. For example, in the protonated form, the nitrogen atom has a positive charge and a smaller lob in the HOMO, while in the deprotonated form, the nitrogen atom has a negative charge and a larger lob in the LUMO. The electron density is more pronounced in regions with larger and same-signed lobs. For instance, in amphetamine's HOMO, electron density concentrates on the nitrogen atom and its double-bond-connected carbon atoms. Conversely, in amphetamine's LUMO, electron density mostly concentrates on its double-bond-connected carbon atoms on a benzene ring. Regions with smaller or oppositely-signed lobs have lower electron density.

4. Conclusions

This work investigated the reactivity, electronic characteristics, and molecular interactions of five different forms of monoamine neurotransmitters: deprotonated, protonated, and neutral. Various quantum chemical methods were used to analyze their structural, energetic, and optical characteristics. The protonation states of these

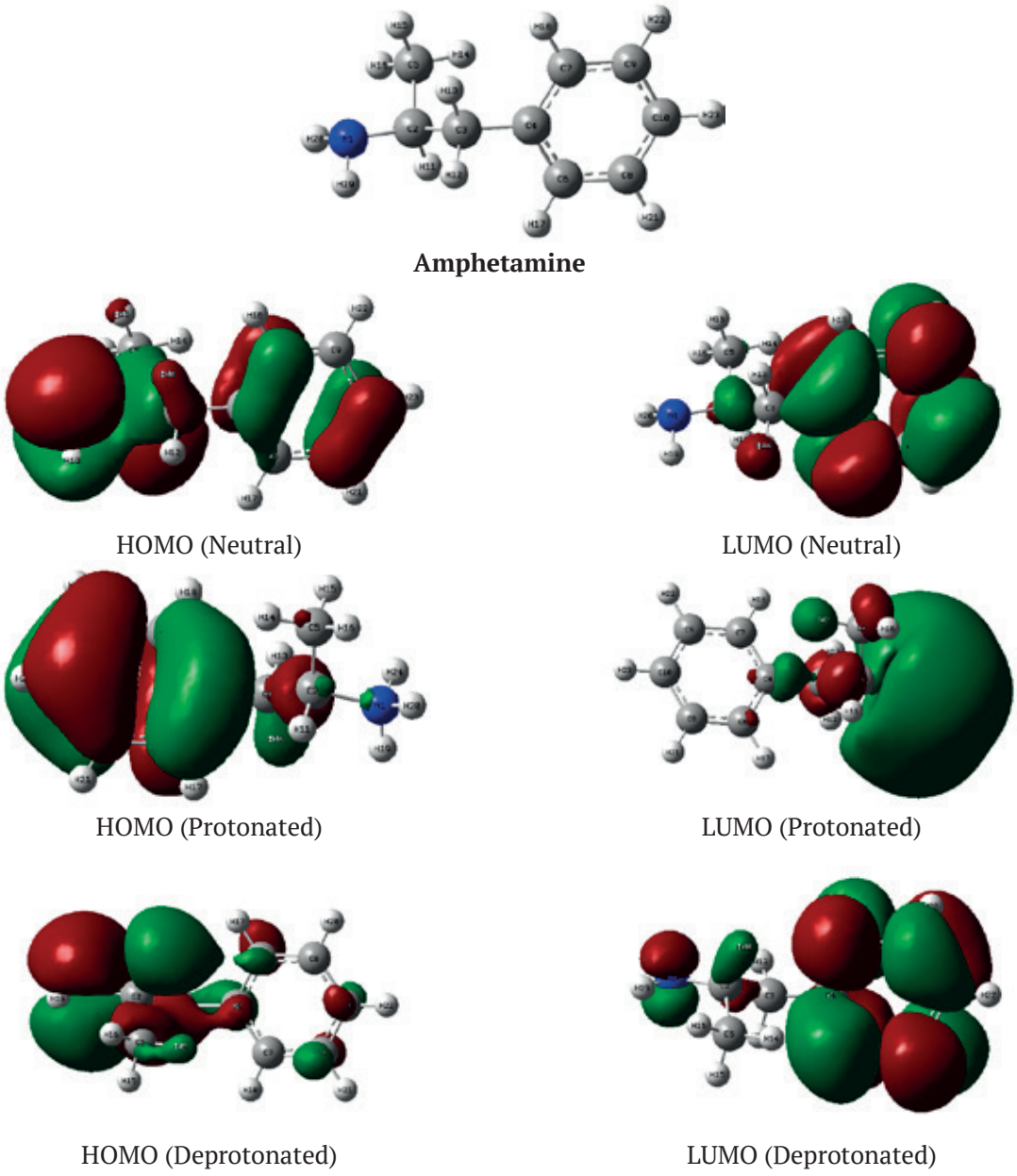

Fig. 5. Optimized structures, HOMO, and LUMO energies for Neutral, -protonated, and deprotonated

compounds changed the weak intermolecular forces and hydrogen bonding patterns that they showed. Lewis structures and NBO analysis were demonstrated to be effective tools for observing their resonance and the motion of the electrons. It was demonstrated that protons added or removed altered the molecular orbitals and energy gaps of these compounds, potentially affecting their reaction. It was also found that their nonlinear optical properties changed depending on their polarizability and hyperpolarizability indices. This meant that they could be used in optical devices. The results provided insights into the molecular mechanisms and functions of these neurotransmitters in the brain and suggested new avenues for their applications in nanotechnology.

Contribution of the authors

The authors contributed equally to this article.

Conflict of interests

The authors declare that they have no known competing financial interests or personal

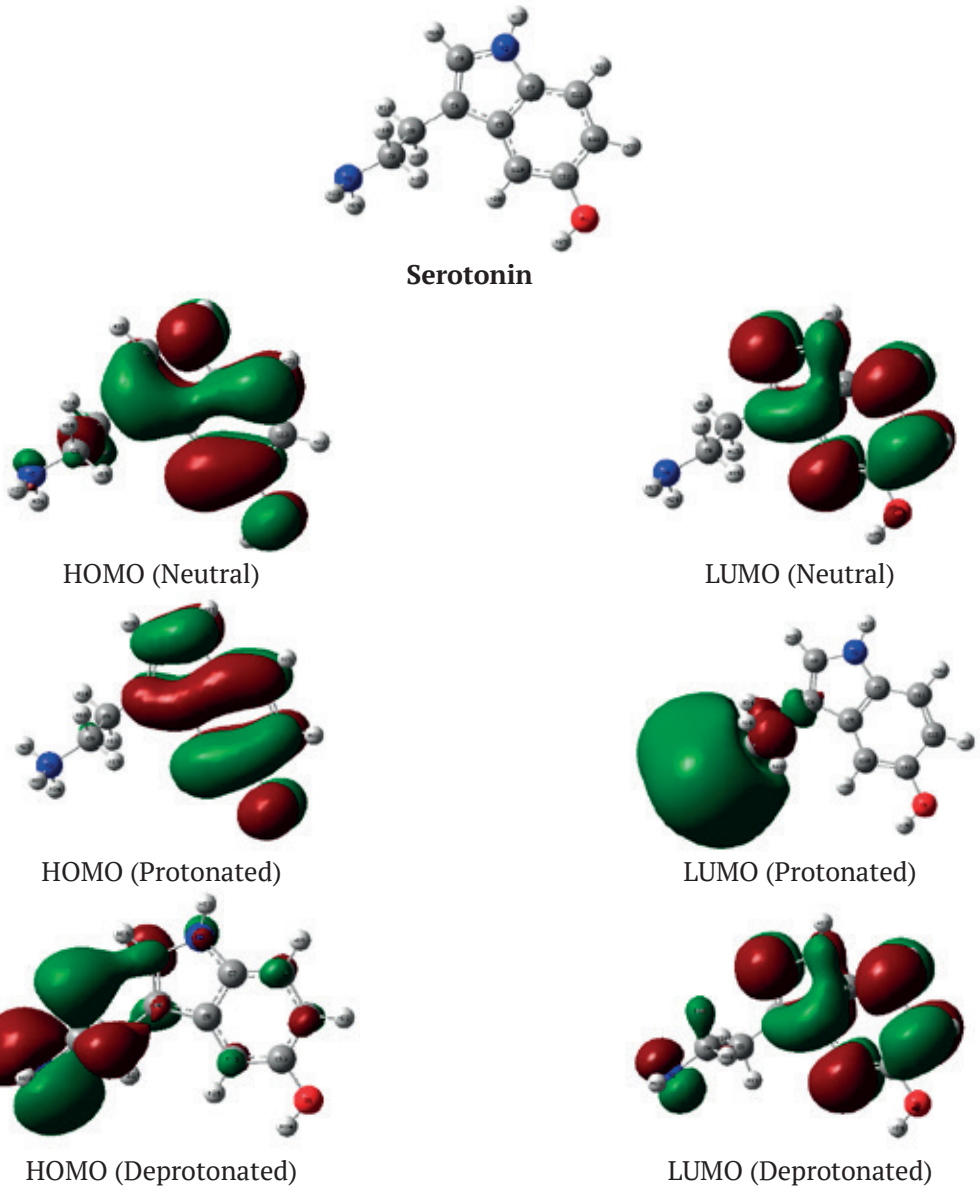

Fig. 6. Optimized structures, HOMO, and LUMO energies for Neutral, -protonated, and deprotonated

relationships that could have influenced the work reported in this paper.

References

1. Fleckenstein A. E., Volz T. J., Riddle E. L., Gibb J. W., Hanson G. R. New insights into the mechanism of action of amphetamines. *Annual Review of Pharmacology and Toxicology*. 2007;47: 681–698. https://doi.org/10.1146/annurev.pharmtox.47.120505.105140

2. Sulzer D., Sonders M. S., Poulsen N. W., Galli A. Mechanisms of neurotransmitter release by amphetamines: a review. *Progress in Neurobiology*. 2005;75: 406–433. https://doi.org/10.1016/j.pneurobio.2005.04.003

3. Kahlig K. M., Binda F., Khoshbouei H., … Galli A. Amphetamine induces dopamine efflux through a dopamine transporter channel. *Proceedings of the National Academy of Sciences*. 2005;102: 3495–3500. https://doi.org/10.1073/pnas.0407737102

4. Gatley S. J., Pan D., Chen R., Chaturvedi G., Ding Y.-S. Affinities of methylphenidate derivatives for dopamine, norepinephrine and serotonin transporters. *Life Sciences*. 1996;58: PL231–PL239. https://doi.org/10.1016/0024-3205(96)00052-5

5. Jones R. S. G. Tryptamine: a neuromodulator or neurotransmitter in mammalian brain? *Progress in Neurobiology*. 1982;19: 117–139. https://doi.org/10.1016/0301-0082(82)90023-5

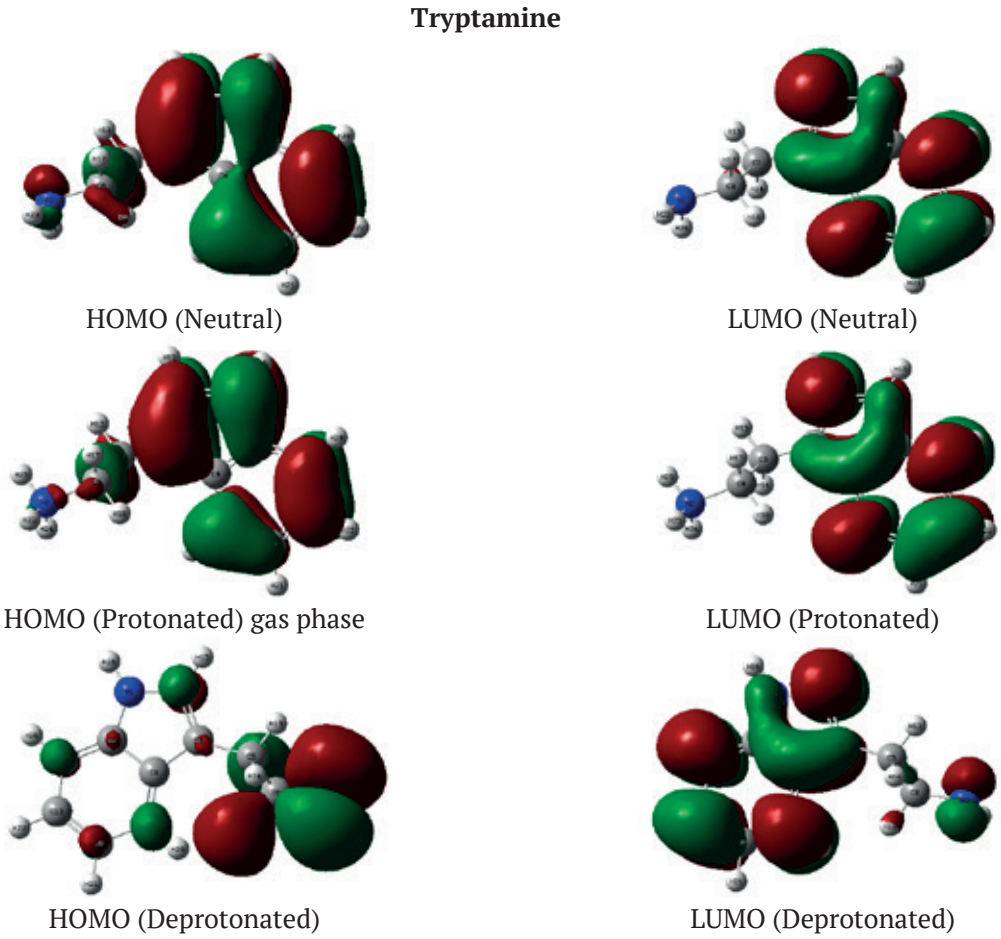

Fig. 7. Optimized structures, HOMO, and LUMO energies for Neutral, protonated, and deprotonated

6. Hobza P., Rezac J. Introduction: noncovalent interactions. *Chemical Reviews*. 2016;116: 4911–4912. https://doi.org/10.1021/acs.chemrev.6b00247

7. Lu T., Chen Q. Independent gradient model based on Hirshfeld partition: A new method for visual study of interactions in chemical systems. *Journal of Computational Chemistry*. 2022;43: 539–555. https://doi.org/10.1002/jcc.26812

8. Raffa R. B., Stagliano G. W., Spencer S. D. Protonation effect on drug affinity. *European Journal of Pharmacology*. 2004;483: 323–324. https://doi.org/10.1016/j.ejphar.2003.10.019

9. Saleh G., Gatti C., Presti L. L. Non-covalent interaction via the reduced density gradient: Independent atom model vs experimental multipolar electron densities. *Computational and Theoretical Chemistry*. 2012;998: 148–163. https://doi.org/10.1016/j.comptc.2012.07.014

10. Parameswari A. R., Rajalakshmi G., Kumaradhas P. A combined molecular docking and charge density analysis is a new approach for medicinal research to understand drug–receptor interaction: Curcumin–AChE model. *Chemico-Biological Interactions*. 2015;225: 21–31. https://doi.org/10.1016/j.cbi.2014.09.011

11. Destro R., Soave R., Barzaghi M., Lo Presti L. Progress in the understanding of drug–receptor interactions. Part 1: experimental charge-density study of an angiotensin II receptor antagonist ($C_{30}H_{30}N_6O_3S$) at T = 17 K. *Chemistry – A European Journal*. 2005;11: 4621–4634. https://doi.org/10.1002/chem.200400964

12. Oliveira V. P., Marcial B. L., Machado F. B., Kraka E. Metal–halogen bonding seen through the eyes of vibrational spectroscopy. *Materials*. 2019;13: 55. https://doi.org/10.3390/ma13010055

13. Chandola P., Dwivedi J., Jamali M. C. Non-linear optical activity and biological evalution of organic compouds by experimental and theoretical techniques. *European Chemical Bulletin*. 2023;12(4): 19608–19619. https://doi.org/10.48047/ecb/2023.12.si4.1741

14. Bhattacharya P. *Nonlinear optical probes for organic field effect transistors and halide perovskites*. Thesis. University of Missouri--Columbia: 2023, 142 p. Available at: https://hdl.handle.net/10355/96071

15. Mamad D. M., Rasul H. H., Awla A. H., Omer R. A. Insight into corrosion inhibition efficiency of imidazole-based molecules: a quantum chemical study. *Doklady Physical Chemistry*. 2023;511(2): 125–133. https://doi.org/10.1134/s0012501623600043

16. Rasul H. H., Mamad D. M., Azeez Y. H., Omer R. A., Omer K. A. Theoretical investigation on corrosion inhibition efficiency of some amino acid compounds *Computational and Theoretical Chemistry*. 2023;1225: 114177. https://doi.org/10.1016/j.comptc.2023.114177

17. Parlak A. E., Omar R. A., Koparir P., Salih M. I. Experimental, DFT and theoretical corrosion study for 4-(((4-ethyl-5-(thiophen-2-yl)-4H-1, 2, 4-triazole-3-yl) thio) methyl)-7, 8-dimethyl-2H-chromen-2-one. *Arabian Journal of Chemistry*. 2022;15: 104088. https://doi.org/10.1016/j.arabjc.2022.104088

18. Steinmann S. N., Corminboeuf C. Exploring the limits of density functional approximations for interaction energies of molecular precursors to organic electronics. *Journal of Chemical Theory and Computation*. 2012;8: 4305–4316. https://doi.org/10.1021/ct300657h

19. Anwar Omar R., Koparir P., Koparir M., Safin D. A. A novel cyclobutane-derived thiazole–thiourea hybrid with a potency against COVID-19 and tick-borne encephalitis: synthesis, characterization, and computational analysis. *Journal of Sulfur Chemistry*. 2023;45(1): 120–137. https://doi.org/10.1080/17415993.2023.2260918

20. Mamad D. M., Omer R. A., Othman K. A. Quantum chemical analysis of amino acids as anti-corrosion agents *Corrosion Reviews*. 2023;41(6), 703–717. https://doi.org/10.1515/corrrev-2023-0031

21. Boukabcha N., Benmohammed A., Belhachemi M. H. M., ... Djafri A. Spectral investigation, TD-DFT study, Hirshfeld surface analysis, NCI-RDG, HOMO-LUMO, chemical reactivity and NLO properties of 1-(4-fluorobenzyl)-5-bromolindolin-2,3-dione. *Journal of Molecular Structure*. 2023;1285: 135492. https://doi.org/10.1016/j.molstruc.2023.135492

22. Omer R. A., Koparir P., Ahmed L. O. Characterization and inhibitor activity of two newly synthesized thiazole. *Journal of Bio-and Tribo-Corrosion*. 2022;8: 28. https://doi.org/10.1007/s40735-021-00625-1

23. Saidj M., Djafri A., Rahmani R., ... Chouaih A. Molecular structure, experimental and theoretical vibrational spectroscopy,(HOMO-LUMO, NBO) investigation,(RDG, AIM) analysis,(MEP, NLO) study and molecular docking of Ethyl-2-{[4-Ethyl-5-(Quinolin-8-yloxyMethyl)-4H-1, 2, 4-Triazol-3-yl] Sulfanyl} acetate. *Polycyclic Aromatic Compounds*. 2023;43: 2152–2176. https://doi.org/10.1080/10406638.2022.2039238

24. Omar R. A., Koparir P., Sarac K., Koparir M., Safin D. A. A novel coumarin-triazole-thiophene hybrid: synthesis, characterization, ADMET prediction, molecular docking and molecular dynamics studies with a series of SARS-CoV-2 proteins. *Journal of Chemical Sciences*. 2023;135(1): 6. https://doi.org/10.1007/s12039-022-02127-0

25. Tang L., Zhu W. Computational design of high energy RDX-based derivatives: property prediction, intermolecular interactions, and decomposition mechanisms. *Molecules*. 2021;26(23): 7199. https://doi.org/10.3390/molecules26237199

26. Jumabaev A., Holikulov U., Hushvaktov H., Issaoui N., Absanov A. Intermolecular interactions in ethanol solution of OABA: Raman, FTIR, DFT, M062X, MEP, NBO, FMO, AIM, NCI, RDG analysis. *Journal of Molecular Liquids*. 2023;377: 121552. https://doi.org/10.1016/j.molliq.2023.121552

27. Bader R. F., Definition of molecular structure: by choice or by appeal to observation? *The Journal of Physical Chemistry A*. 2010;114: 7431–7444. https://doi.org/10.1021/jp102748b

28. Rozas I., Alkorta I., Elguero J. Behavior of ylides containing N, O, and C atoms as hydrogen bond acceptors. *Journal of the American Chemical Society*. 2000;122: 11154–11161. https://doi.org/10.1021/ja0017864

29. Omer R. A., Koparir P., Ahmed L. Theoretical determination of corrosion inhibitor activities of 4-allyl-5-(pyridin-4-yl)-4H-1, 2, 4-triazole-3-thiol-thione tautomerism. *Indian Journal of Chemical Technology (IJCT)*. 2022;29: 75–81. https://doi.org/10.56042/ijct.v29i1.51231

30. Omer R., Koparir P., Koparir M., Rashid R., Ahmed L., Hama J. Synthesis, characterization and DFT study of 1-(3-Mesityl-3-methylcyclobutyl)-2-((4-phenyl-5-(thiophen-2-yl)-4H-1, 2, 4-triazol-3-yl) thio) ethan-1-one. *Protection of Metals and Physical Chemistry of Surfaces*. 2022;58: 1077–1089. https://doi.org/10.1134/s2070205122050185

31. Sandhu B., McLean A., Sinha A. S., ...Aakeröy C. B. Evaluating competing intermolecular interactions through molecular electrostatic potentials and hydrogen-bond propensities. *Crystal Growth & Design*. 2018;18: 466–478. https://doi.org/10.1021/acs.cgd.7b01458

32. Clark D. E. What has polar surface area ever done for drug discovery? *Future Medicinal Chemistry*. 2011;3: 469–484. https://doi.org/10.4155/fmc.11.1

33. Lipinski C. A. Drug-like properties and the causes of poor solubility and poor permeability. *Journal of Pharmacological and Toxicological Methods*. 2000;44: 235–249. https://doi.org/10.1016/s1056-8719(00)00107-6

34. Jain A. N. Surflex: fully automatic flexible molecular docking using a molecular similarity-based search engine. *Journal of Medicinal Chemistry*. 2003;46: 499–511. https://doi.org/10.1021/jm020406h

35. Silberstein L. L. Molecular refractivity and atomic interaction. II. *The London, Edinburgh, and Dublin Philosophical Magazine and Journal of Science*. 1917;3(198): 521–533. https://doi.org/10.1080/14786440608635666

36. Ranjith P., Ignatious A., Panicker C. Y., ... Anto P. Spectroscopic investigations, DFT calculations, molecular docking and MD simulations of 3-[(4-Carboxyphenyl) carbamoyl]-4-hydroxy-2-oxo-1, 2-dihydroxy quinoline-6-carboxylic acid. *Journal of Molecular Structure*. 2022;1264: 133315. https://doi.org/10.1016/j.molstruc.2022.133315

37. Sumathi D., Thanikachalam V., Bharanidharan S., Saleem H., Babu N. R. Vibrational spectroscopy (FT-IR, FT-Raman and UV) studies of E-[1-Methyl-2, 6-diphenyl-3-(propan-2-yl) piperidin-4-ylidene] amino 3-methylbenzoate] using DFT method. *International Journal of Scientific Reseach*. 2016;5(3): 694-713. Available at: https://www.worldwidejournals.com/international-journal-of-scientific-research-(IJSR)/fileview.php?val=March_2016_1492757409__217.pdf

38. Abbaz T., Bendjeddou A., Villemin D. Structure, electronic properties, NBO, NLO and chemi-cal reactivity of bis (1, 4-dithiafulvalene) derivatives: functional density theory study. *International Journal of Advanced Chemistry*. 2017;6: 18–25. https://doi.org/10.14419/ijac.v6i1.8668

39. Villemin D., Abbaz T., Bendjeddou A. Molecular structure, HOMO, LUMO, MEP, natural bond orbital analysis of benzo and anthraquinodimethane derivatives. *Pharmaceutical and Biological Evaluations*. 2018;5(2), 27. https://doi.org/10.26510/2394-0859.pbe.2018.04

40. Abbaz T., Bendjeddou A., Villemin D. Molecular structure, NBO analysis, first hyper polarizability, and homo-lumo studies of π-extended tetrathiafulvalene (EXTTF) derivatives connected to π-nitro phenyl by density functional method. *International Journal of Advanced Chemistry*. 2018;6(1), 114–120. https://doi.org/10.14419/ijac.v6i1.11126

41. Rebaz O., Ahmed L., Koparir P., Jwameer H. Impact of solvent polarity on the molecular properties of dimetridazole. *El-Cezeri Fen ve Mühendislik Dergisi*. 2022;9: 740–747. https://doi.org/10.31202/ecjse.1000757

42. Khan M. U., Khalid M., Asim S., ... Imran M. Exploration of nonlinear optical properties of triphenylamine-dicyanovinylene coexisting donor-π-acceptor architecture by the modification of π-conjugated linker. *Frontiers in Materials*. 2021;8: 719971. https://doi.org/10.3389/fmats.2021.719971

43. Al-Shamiri H. A., Sakr M. E., Abdel-Latif S. A., ... Elwahy A. H. Experimental and theoretical studies of linear and non-linear optical properties of novel fused-triazine derivatives for advanced technological applications. *Scientific Reports*. 2022;12: 19937. https://doi.org/10.1038/s41598-022-22311-z

44. Atlam F. M., Awad M. K., El-Bastawissy E. A. Computational simulation of the effect of quantum chemical parameters on the molecular docking of HMG-CoA reductase drugs. *Journal of Molecular Structure*. 2014;1075: 311–326. https://doi.org/10.1016/j.molstruc.2014.06.045

45. Oldfield E. Chemical shifts in amino acids, peptides, and proteins: from quantum chemistry to drug design *Annual Review of Physical Chemistry*. 2002;53: 349–378. https://doi.org/10.1002/chin.200249272

46. Gallo M., Favila A., Glossman-Mitnik D. DFT studies of functionalized carbon nanotubes and fullerenes as nanovectors for drug delivery of antitubercular compounds. *Chemical Physics Letters*. 2007;447: 105–109. https://doi.org/10.1016/j.cplett.2007.08.098

47. Akbas E., Othman K. A., Çelikezen F. Ç., ... Mardinoglu A. Synthesis and biological evaluation of novel benzylidene thiazolo pyrimidin-3(5H)-one derivatives. *Polycyclic Aromatic Compounds*. 2023; 1–18. https://doi.org/10.1080/10406638.2023.2228961

48. Al-Fahemi J. H., Abdallah M., Gad E. A., Jahdaly B., Experimental and theoretical approach studies for melatonin drug as safely corrosion inhibitors for carbon steel using DFT. *Journal of Molecular Liquids*. 2016; 222: 1157–1163. https://doi.org/10.1016/j.molliq.2016.07.085

49. Bani-Yaseen A. D. Investigation on the impact of solvent on the photochemical properties of the photoactive anticancer drug Vemurafenib: a computational study. *Journal of Molecular Liquids*. 2021;322: 114900. https://doi.org/10.1016/j.molliq.2020.114900

50. Sustmann R. Orbital energy control of cycloaddition reactivity. *Physical Organic Chemistry–2*. 1974; 569–593. https://doi.org/10.1016/b978-0-408-70681-0.50009-9

51. Perveen M., Nazir S., Arshad A. W., ... Iqbal J. Therapeutic potential of graphitic carbon nitride as a drug delivery system for cisplatin (anticancer drug): a DFT approach. *Biophysical Chemistry*. 2020;267: 106461. https://doi.org/10.1016/j.bpc.2020.106461

52. Jaffar K., Riaz S., Afzal Q. Q., ... Al-Buriahi M. A DFT approach towards therapeutic potential of phosphorene as a novel carrier for the delivery of felodipine (cardiovascular drug). *Computational and Theoretical Chemistry*. 2022;1212: 113724. https://doi.org/10.1016/j.comptc.2022.113724

53. Lewis D. F. Frontier orbitals in chemical and biological activity: quantitative relationships and

mechanistic implications. *Drug Metabolism Reviews*. 1999;31: 755–816. https://doi.org/10.1081/dmr-100101943

Information about the authors

Yousif Hussein Azeez, MSc in Advanced Materials Science, Lecturer at the Department of physics, Halabja University (Iraq).
https://orcid.org/0000-0001-5357-7856
yousif.husain@uoh.edu.iq

Khdir Ahmed Othman, MSc In Organic Chemistry, Lecturer at the Department of Chemistry, Faculty of Science and Health, Koya University, (Kurdistan Region – F.R., Iraq).
https://orcid.org/0000-0002-7763-2976
khdir.ahmed@koyauniversity.org

Rebaz Anwar Omer, PhD in Organic Chemistry, Head of Chemistry Department, Faculty of Science and Health, Koya University (Kurdistan Region – F.R., Iraq), Department of Pharmacy, College of Pharmacy, Knowledge University (Erbil, Iraq).
https://orcid.org/0000-0002-3774-6071
rebaz.anwar@koyauniversity.org

Aryan Fathulla Qader, PhD in Analytical Chemistry, Lecturer at the Departmet of Chemistry, Faculty of Science and Health, Koya University (Kurdistan Region – F.R., Iraq).
https://orcid.org/0000-0002-2547-7708
aryan.qader@koyauniversity.org

Received 28.10.2023; approved after reviewing 22.12.2023; accepted for publication 15.01.2024; published online 01.10.2024.